Synthesis and Biological Characterization of 1,4,5,6-Tetrahydropyrimidine and 2-Amino-3,4,5,6-tetrahydropyridine Derivatives as Selective m1 Agonists

William S. Messer, Jr.,* Yahaya F. Abuh, Yang Liu, Sumudra Periyasamy,† Dan O. Ngur, Michael A. N. Edgar,‡ Afif A. El-Assadi, Sbeih Sbeih, Philip G. Dunbar,§ Scott Roknich, Taikyun Rho, Zheng Fang, Babatunde Ojo,⊥ Hao Zhang,|| James J. Huzl, III, and Peter I. Nagy

Center for Drug Design and Development, Department of Medicinal & Biological Chemistry, College of Pharmacy, The University of Toledo, 2801 West Bancroft Street, Toledo, Ohio 43606

Received June 28, 1996[⊗]

Previous studies identified several novel tetrahydropyrimidine derivatives exhibiting muscarinic agonist activity in rat brain. Such compounds might be useful in treating cognitive and memory deficits associated with low acetylcholine levels, as found in Alzheimer's disease. To determine the molecular features of ligands important for binding and activity at muscarinic receptor subtypes, the series of tetrahydropyrimidines was extended. Several active compounds were examined further for functional selectivity through biochemical studies of muscarinic receptor activity using receptor subtypes expressed in cell lines. Several amidine derivatives displayed high efficacy at m1 receptors and lower activity at m3 receptors coupled to phosphoinositide (PI) metabolism in A9 L cells. Four ligands, including **1b**, **1f**, **2b**, and **7b**, exhibited marked functional selectivity for m1 vs m3 receptors. Compound **1f** also exhibited low activity at m2 receptors coupled to the inhibition of adenylyl cyclase in A9 L cells. Molecular modeling studies also were initiated to help understand the nature of the interaction of muscarinic agonists with the m1 receptor using a nine amino model of the m1 receptor. Several important interactions were identified, including interactions between the ester moiety and Thr192. Additional interactions were found for oxadiazoles and alkynyl derivatives with Asn382, suggesting that enhanced potency and selectivity may be achieved by maximizing interactions with Asp105, Thr192, and Asn382. Taken together, the data indicate that several amidine derivatives display functional selectivity for m1 muscarinic receptors, warranting further evaluation as therapeutic agents for the treatment of Alzheimer's disease. In addition, several amino acid residues were identified as potential binding sites for m1 agonists. These data may be useful in directing efforts to develop even more selective m1 agonists.

Alzheimer's disease is associated with a loss of the basal forebrain neurons that release acetylcholine in the cerebral cortex and hippocampus.[1−4] Decreased levels of acetylcholine may account for the memory deficits and cognitive dysfunction associated with the early stages of the progressive disorder. Acetylcholinesterase inhibitors (e.g., physostigmine, tacrine) have been utilized to elevate acetylcholine levels and treat the symptoms of Alzheimer's disease, yet provide limited therapeutic benefit, in part due to the high incidence of undesirable side effects and the progressive loss of the target enzyme.[5,6]

Over the past decade, drug development efforts have focused on identifying muscarinic agonists that directly activate receptors on postsynaptic neurons.[7,8] Four subtypes of muscarinic receptor have been identified on the basis of pharmacological studies (designated M_1−M_4), while molecular biological studies have identified five muscarinic receptor subtypes (m1−m5). On the basis of the preferential localization of M_1 muscarinic receptors in the hippocampus and cerebral cortex,[9−14] and their involvement in memory function,[15−18] the search has focused on selective M_1 agonists. Such ligands would selectively activate receptors coupled to phosphoinositide metabolism in the cerebral cortex and hippocampus[19−21] without decreasing acetylcholine levels by activating central M_2 receptors[22−25] or activating peripheral M_2 receptors involved in regulating cardiac function[26,27] and M_3 receptors associated with increased gastrointestinal and exocrine gland activity.[27,28]

Over the past few years, several novel amidine derivatives have been synthesized and tested for muscarinic agonist activity in rat brain.[19−31] Several compounds stimulated muscarinic receptors coupled to PI metabolism in the cerebral cortex and hippocampus, including the methyl (**1a**), ethyl (**1b**), and propargyl (**1f**) esters of 1,4,5,6-tetrahydropyrimidine, the methyl- and ethyl-1,2,4-oxadiazole derivatives (**2a** and **2b**, respectively) of 1,4,5,6-tetrahydropyrimidine, and the methyl (**7a**, **8a**) and propargyl (**7b**, **8b**) esters of racemic 2-amino-3,4,5,6-tetrahydropyridine and 2-amino-1,4,5,6-tetrahydropyrimidine, respectively.

The series of amidine derivatives was extended through replacement of the ester moiety and modification of the alkyl functionality and tested for muscarinic agonist activity in rat brain. Several compounds displaying promising muscarinic agonist activity were studied further to determine their selectivities for m1 receptors and their potential as therapeutic agents for the treatment of Alzheimer's disease. Agonist activity was determined at m1, m2, and m3 receptors expressed

† Present address: Medical College of Ohio, P.O. Box 10008, Toledo, OH 43699.
‡ Present address: Rudolf Magnus Institute For Neurosciences, 100 Universiteitsweg, 3584 CG Utrecht, The Netherlands.
§ Present address: Washington State University, Health Research and Education Center, W. 601st Avenue, Spokane, WA 99204.
⊥ Present address: Georgia Institute Of Technology, School Of Chemistry and Biochemistry, Gilbert H. Boggs Building, Room 3-8, Atlanta, GA 30332-0400.
|| Present address: Bristol Myers Squibb Institute, P.O. Box 4000, H12-03, Princeton, NJ 08543-4000.
⊗ Abstract published in *Advance ACS Abstracts,* March 15, 1997.

S0022-2623(96)00467-0 CCC: $14.00

Chart 1

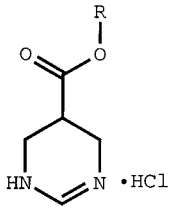

R	#
Methyl	**1a**
Ethyl	**1b**
Isopropyl	**1c**
2-Methylbutyl	**1d**
3-Methylbutyl	**1e**
Propargyl	**1f**
2-Butynyl	**1g**
Butynyl	**1h**
3-pentynyl	**1i**
2-pentynyl	**1j**
pentynyl	**1k**
trans-3-methyl-2-penten-4-ynyl	**1l**
cis-3-methyl-2-penten-4-ynyl	**1m**
3-penten-1-ynyl	**1n**
2-methylbutenyl	**1o**
3-methylpropynyl	**1p**
3-dimethylpropynyl	**1q**
phenylpropynyl	**1r**
propenyl	**1s**

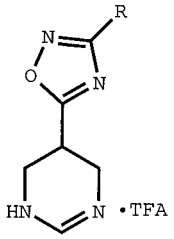

R	#
Methyl	**2a**
Ethyl	**2b**
Isopropyl	**2c**
2-Methylpropyl	**2d**
2-Methylbutyl	**2e**
Butynyl	**2f**
Pentynyl	**2g**
Methyloxymethyl	**2h**
Ethyloxymethyl	**2i**
Ethyloxyethyl	**2j**
Methylthiomethyl	**2k**

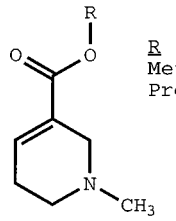

R	#
Methyl	**3a** (arecoline)
Propargyl	**3b** (APE)

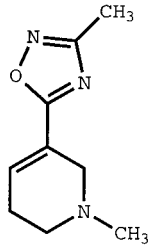

4

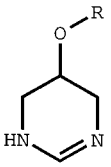

R	#
Methyl	**5a**
Propargyl	**5b**

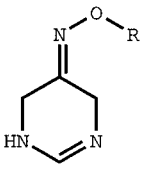

R	#
Methyl	**6a**
Ethyl	**6b**
Phenylpropynyl	**6c**

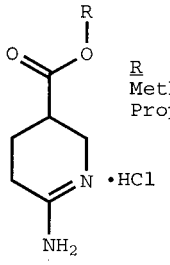

R	#
Methyl	**7a**
Propargyl	**7b**

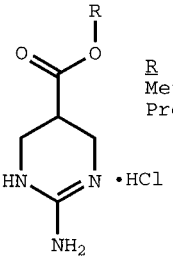

R	#
Methyl	**8a**
Propargyl	**8b**

in A9 L cells through biochemical assays of PI metabolism and cAMP formation. The data indicate that several amidine derivatives display functional selectivity for m1 muscarinic receptors, warranting further evaluation as therapeutic agents for the treatment of Alzheimer's disease.

Results

Synthetic Chemistry. The first series of tetrahydropyrimidine esters (**1d** and **1e**) was synthesized by esterification of the reduced acid according to literature procedures.[29,30] The remaining esters (**1g**−**s**) were prepared by first forming the acid chloride using a solution of oxalyl chloride in benzene and then reacting this with the desired alkynols (see Scheme 1).

A series of branched alkyl- and alkynyloxadiazole derivatives of tetrahydropyrimidine (**2c**−**k**) was also synthesized using an extension of a variety of literature procedures.[30,32,33] An efficient single-vessel reaction of the appropriately substituted amide oximes[32] with 1 equiv of sodium hydride in refluxing dry THF led to the corresponding anions, which, after addition of the trityl-protected tetrahydropyrimidine ester, cyclized to the 5-oxadiazole-substituted tetrahydropyrimidine derivatives. Deprotection of the *N*-trityltetrahydropyrimidine oxadiazole with trifluoroacetic acid (TFA) gave the desired products (**2c**−**k**) as TFA salts (Scheme 2).[30]

Scheme 1

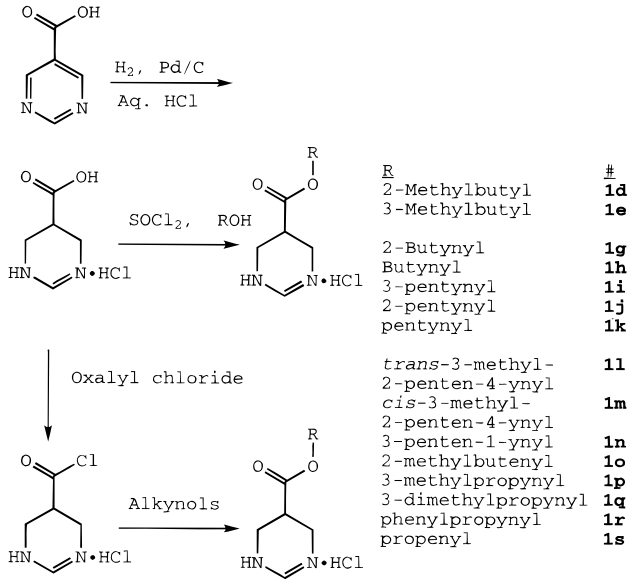

R	#
2-Methylbutyl	**1d**
3-Methylbutyl	**1e**
2-Butynyl	**1g**
Butynyl	**1h**
3-pentynyl	**1i**
2-pentynyl	**1j**
pentynyl	**1k**
trans-3-methyl-2-penten-4-ynyl	**1l**
cis-3-methyl-2-penten-4-ynyl	**1m**
3-penten-1-ynyl	**1n**
2-methylbutenyl	**1o**
3-methylpropynyl	**1p**
3-dimethylpropynyl	**1q**
phenylpropynyl	**1r**
propenyl	**1s**

Scheme 2

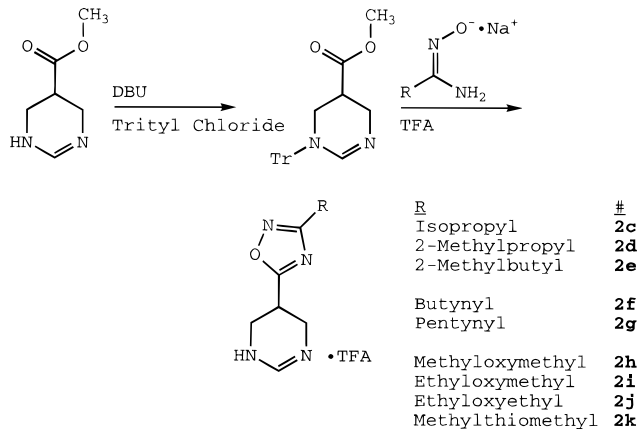

R	#
Isopropyl	**2c**
2-Methylpropyl	**2d**
2-Methylbutyl	**2e**
Butynyl	**2f**
Pentynyl	**2g**
Methyloxymethyl	**2h**
Ethyloxymethyl	**2i**
Ethyloxyethyl	**2j**
Methylthiomethyl	**2k**

Scheme 3

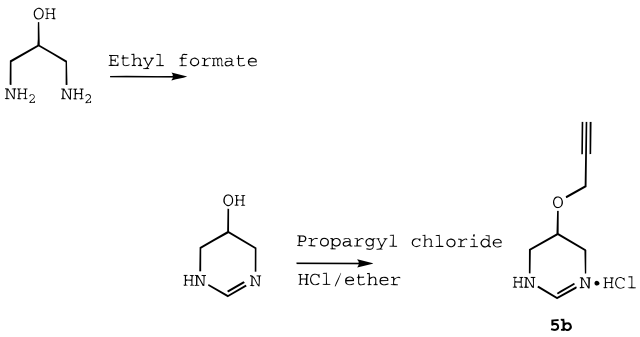

4-Cyanobutyne, which served as a starting material for the oxadiazole **2f**, was prepared from the corresponding alcohol according to the method of Brandsma.[33] 3-Butyn-1-ol was reacted with *p*-toluenesulfonyl chloride to obtain the tosylate, followed by reaction with sodium cyanide in DMSO to give the corresponding nitrile using an extension of literature procedures.[33] The nitrile was converted to its amide oxime,[32] followed by reaction with trityl ester to form the oxadiazole (**2f**), employing a method virtually identical to that used for **2a**−**e** (Scheme 2).

The tetrahydropyrimidine ether derivative (**5b**) was synthesized from the reduced alcohol. 1,4,5,6-Tetrahydro-5-hydroxypyrimidine[34,35] was reacted with propargyl chloride in the presence of potassium carbonate to give the propargyl ether derivative as the free base, which then was converted to the hydrochloride salt (Scheme 3).

A series of tetrahydropyrimidine oxime derivatives (**6a**−**c**) was synthesized from the reduced ketone using an extension of a literature procedure.[36,37] As shown in Scheme 4, 5-hydroxy-1,4,5,6-tetrahydropyrimidine was oxidized to 1,4,5,6-tetrahydropyrimidin-5-one by reacting the alcohol with a suspension of pyridinium chlorochromate in dichloromethane. The ketone was then reacted with the desired alkoxylamine according to literature procedures.[36,37]

Receptor Binding and PI Metabolism in Rat Brain. Muscarinic receptor binding and agonist activity were examined in rat brain tissues in preliminary fashion for all new ligands. Receptor binding affinity was assessed through inhibition of specific [^{3}H]-(*R*)-QNB binding to rat brain membranes. Several novel ligands exhibited high affinity (IC_{50} values < 10 μM) for muscarinic receptors in rat brain, as shown in Table 1. Ester derivatives with the highest affinity included **1l**, **1m**, and **1r**. All oxadiazole derivatives, with the exception of butynyl (**2f**), displayed high potency for muscarinic receptors in rat brain. The ether (**5a** and **5b**) and oxime (**6a**, **6b** and **6c**) derivatives displayed much lower potency with only **5b** exhibiting an IC_{50} value less than 100 μM.

Scheme 4

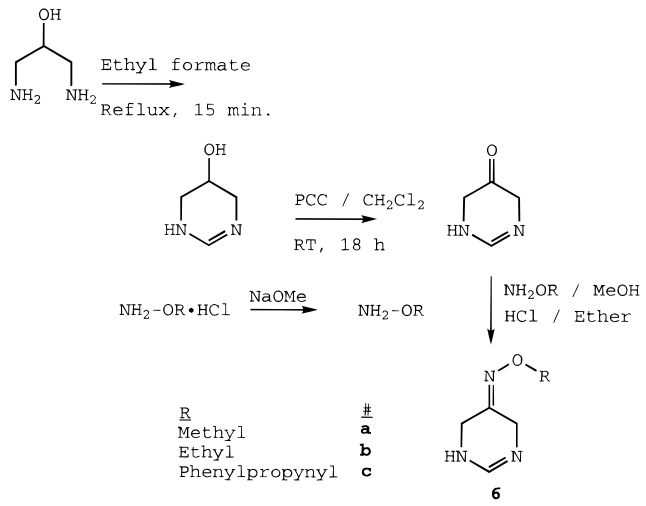

R	#
Methyl	**a**
Ethyl	**b**
Phenylpropynyl	**c**

All compounds with moderate affinity (IC_{50} values < 100 μM) for muscarinic receptors in the rat brain were tested further for agonist activity through assays of PI metabolism in slices from rat cerebral cortex. Several compounds displayed agonist activity in the PI assay, including the butynyl esters **1g** and **1h**, the 2-methylbutyl oxadiazole derivative **2e**, the butynyl oxadiazole derivative **2f**, and the ether and thioether oxadiazoles **2h**−**k**. None of the ether or oxime derivatives exhibited agonist activity in the rat brain.

Receptor Binding in Cell Lines. Cell lines expressing a single subtype of muscarinic receptor provided a suitable measure of muscarinic agonist affinity, activity, and selectivity. Ligand affinity for muscarinic receptor subtypes was determined through inhibition of specific [^{3}H]-(*R*)-QNB binding to m1, m2, or m3 receptors expressed in A9 L cells. Examples from the tetrahydropyrimidine and tetrahydropyridine series of ligands were selected for binding studies to permit a comparison of the relative contributions of the different functional groups to agonist affinity.

As shown in Table 2, each cell line displayed a different level of muscarinic receptors, with m3 > m1 > m2. Inhibition studies revealed that carbachol exhibited highest affinity for m2 receptors (see Figure 1), and binding curves reflected an interaction with multiple receptor states. All other agonists examined also displayed the highest affinity for m2 receptors, as can be seen in Tables 3−5.

As shown in Figures 1−5 and Table 3, the inhibition curves for carbachol, **1a**, and **2a** were biphasic at m1 receptors expressed in A9 L cells. Arecoline and **4** appeared to bind to a single population of m1 receptors. The nonhydrolyzable GTP analog, GTP-γ-S, lowered agonist affinity at m1 receptors. Binding isotherms for carbachol, **1a**, and **2a** in the presence of GTP-γ-S were consistent with a single low-affinity binding site.

The binding of [^{3}H]-(*R*)-QNB, carbachol, and arecoline to m1 muscarinic receptors expressed in A9 L cells was similar to that reported previously,[38] and consistent with similar studies using brain membranes.[39] At each

Table 1. Binding Affinities and Agonist Activity in a Series of Ester (**1**), 1,2,4-Oxadiazole (**2**), Ether (**5**), and Oxime (**6**) Derivatives at Muscarinic Receptors in the Rat Central Nervous System[a]

functionality (R)	ligand	IC_{50} (μM) [^{3}H]QNB	PI cortex (% at 100 μM)
	carbachol	5.5 ± 1.0	470 ± 81
	arecoline	1.0 ± 0.25	110 ± 21
	pilocarpine	7.6 ± 4.4	58 ± 5.6
	aceclidine	0.51 ± 0.10	80 ± 17
methyl	**1a**	9.2 ± 1.9	112 ± 11
ethyl	**1b**	2.2 ± 0.28	150 ± 17
isopropyl	**1c**	3.3 ± 0.12	7.2 ± 3.0
2-methylbutyl	**1d**	21 ± 2.2	−3.0 ± 2.0
3-methylbutyl	**1e**	15 ± 3.0	2.0 ± 3.0
propargyl	**1f**	3.3 ± 0.80	230 ± 35
2-butynyl	**1g**	13 ± 2.7	140 ± 4.1
butynyl	**1h**	14 ± 2.8	100 ± 15
pentynyl	**1i**	14 ± 2.4	−4.0 ± 1.5
2-pentynyl	**1j**	72 ± 9.8	−5.8 ± 4.3
3-pentynyl	**1k**	>100	5.8 ± 7.0
trans-3-methyl-2-penten-4-ynyl	**1l**	4.1 ± 0.63	35 ± 5.6
cis-3-methyl-2-penten-4-ynyl	**1m**	1.5 ± 0.42	50 ± 4.3
3-penten-1-ynyl	**1n**	70 ± 20	7.8 ± 1.6
2-methylbutenyl	**1o**	38 ± 16	24 ± 12
3-methylpropynyl	**1p**	43 ± 2.8	22 ± 3
3,3-dimethylpropynyl	**1q**	>100	
phenylpropynyl	**1r**	9.3 ± 1.5	23 ± 8.2
propenyl	**1s**	12 ± 5.2	21 ± 12
methyl	**2a**	2.7 ± 0.69	700 ± 99
ethyl	**2b**	1.0 ± 0.32	130 ± 16
isopropyl	**2c**	5.3 ± 0.68	60 ± 13
2-methylpropyl	**2d**	1.4 ± 0.12	38 ± 11
2-methylbutyl	**2e**	6.1 ± 0.38	180 ± 60
butynyl	**2f**	16 ± 6.9	130 ± 18
pentynyl	**2g**	2.3 ± 1.2	42 ± 13
methoxymethyl	**2h**	4.0 ± 1.5	110
ethoxymethyl	**2i**	5.1	100
ethoxyethyl	**2j**	2.6 ± 1.3	100
(methylthio)methyl	**2k**	5.1 ± 4.8	180 ± 79
methyl	**5a**	>100	
propargyl	**5b**	32 ± 21	−3.0
methyl	**6a**	>100	
ethyl	**6b**	>100	
phenylpropynyl	**6c**	>100	

[a] Data represent the mean (±sem, where indicated) from one to three experiments, each performed in triplicate. Data for carbachol, arecoline, pilocarpine, aceclidine, **1a**, **1b**, **1c**, **1f**, **2a**, and **2b** have been reported previously and are shown here for comparison.[29,30]

Table 2. Binding of [^{3}H]-(*R*)-QNB to Muscarinic Receptor Subtypes Expressed in A9 L Cells[a]

receptor subtype	B_{max} (fmol/mg)	K_d (pM)
m1	280 ± 50	43 ± 3.7
m2	59 ± 7.9	24 ± 0.77
m3	1500 ± 100	68 ± 4.3

[a] Data represent the mean (±sem) from three assays each performed in triplicate.

muscarinic receptor subtype, carbachol displayed a complex interaction suggesting multiple receptor affinity states. As expected, GTP-γ-S decreased agonist affinity for m1 receptors, and the magnitude of the shift, which has been postulated to reflect agonist efficacy,[39] differed for each ligand. Carbachol, generally considered a full agonist, had a 3-fold shift in affinity, while arecoline displayed a much smaller shift. GTP-γ-S decreased the affinity of both **1a** and **2a** in a similar fashion to carbachol, suggesting that the 1,4,5,6-tetrahydropyrimidine derivatives were able to induce m1 receptor coupling to G-proteins, which was confirmed by studies of PI metabolism. The predicted efficacies obtained from GTP-γ-S shift assays were in excellent agreement with the results of the PI metabolism assays. That is, carbachol and the two 1,4,5,6-tetrahydropyrimidine derivatives appeared to be efficacious agonists at m1 receptors with significantly higher activity than either arecoline or **4**.

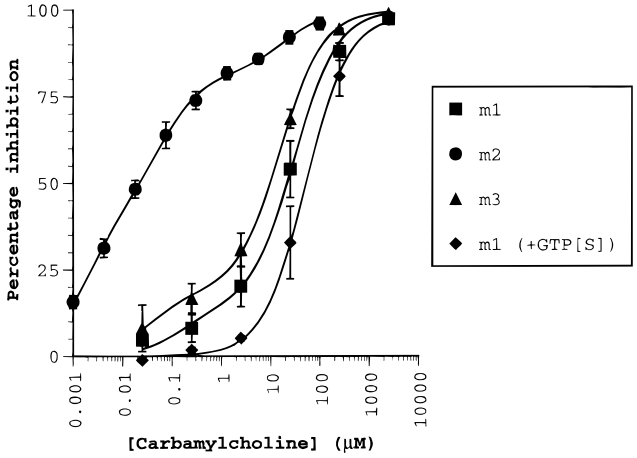

Figure 1. Inhibition of [^{3}H]-(*R*)-QNB binding to m1, m2, and m3 receptors expressed in A9 L cells by carbachol in the absence of GTP-γ-S (GTP[S]). Also shown is the inhibition of the binding [^{3}H]-(*R*)-QNB to m1 receptors by carbachol in presence of 300 μM GTP-γ-S. Data represent the mean (±sem) from three experiments, each performed in triplicate.

Carbachol displayed the highest affinity for m2 receptors (vs m1 or m3 receptors), in agreement with previous studies.[40] The percentage of m2 receptors with high agonist affinity suggests more efficient coupling of m2 receptors to G-proteins than either m1 or m3 receptors. In contrast, agonist binding to low-affinity sites was comparable at m1, m2, and m3 receptors. These data

Table 3. Inhibition of [^{3}H]-(*R*)-QNB Binding to m1 Receptors Expressed in A9 L Cells by Several Muscarinic Agonists in the Absence and Presence of 300 μM GTP-γ-S[a]

	−GTP-γ-S				+GTP-γ-S	
ligand	% high	K_i High (nM)	% low	K_i low (μM)	% binding	K_i (μM)
carbachol	16.5 ± 3.13	739 ± 668	83.4 ± 3.13	19.9 ± 6.60	99.8 ± 0.841	37.1 ± 15.4
arecoline			99.4 ± 1.17	3.33 ± 0.554	101 ± 0.820	5.45 ± 0.900
4			98.5 ± 0.642	0.589 ± 0.0550	100 ± 0.325	1.05 ± 0.144
1a	23.5 ± 5.25	359 ± 95.7	76.5 ± 5.25	23.6 ± 1.47	97.9 ± 0.726	26.8 ± 1.73
1f	31.5 ± 7.43	41.7 ± 32.9	68.5 ± 7.43	2.88 ± 0.104		
1g	23.4 ± 3.45	14.0 ± 2.64	76.6 ± 3.45	9.01 ± 2.07		
1h	23.2 ± 2.15	30.9 ± 15.0	76.8 ± 2.15	15.5 ± 3.73		
2a	30.9 ± 1.70	21.1 ± 4.61	69.1 ± 1.70	2.31 ± 0.333	98.3 ± 0.529	2.50 ± 0.657
2g	32.5 ± 2.80	138 ± 108	67.5 ± 2.80	17.4 ± 1.57		

[a] Data represent the mean (±sem) percentage of binding sites and K_i values for each site. K_i values were calculated using IC_{50} values obtained by nonlinear curve fitting, accordingv to the best fit ($p < 0.05$) of the binding data to a one- or two-site model. The data are from three separate binding assays, each determined in triplicate.

Table 4. Inhibition of [^{3}H]-(*R*)-QNB Binding to m2 Receptors Expressed in A9 L Cells by Several Muscarinic Agonists[a]

ligand	% high	K_H (nM)	% medium	K_M (nM)	% low	K_L (μM)
carbachol	43 ± 6.7	0.81 ± 0.34	40 ± 5.0	46 ± 31	17 ± 1.9	12 ± 5.9
1a			70 ± 2.4	14 ± 3.6	30 ± 2.4	3.3 ± 0.58
2a			66 ± 5.0	1.1 ± 0.52	34 ± 5.0	0.46 ± 0.28
arecoline			65 ± 2.7	2.4 ± 0.33	35 ± 2.7	0.56 ± 0.054
4			60 ± 2.4	0.94 ± 0.22	40 ± 2.4	0.087 ± 0.047

[a] Data represent the mean (±sem) percentage of binding sites and K_i values for each site. K_i values were calculated using IC_{50} values obtained by nonlinear curve fitting, according to the best fit ($p < 0.05$) of the binding data to a one-, two-, or three-site model. The data are from three separate binding assays, each determined in triplicate.

Table 5. Inhibition of [^{3}H]-(*R*)-QNB Binding to m3 Receptors Expressed in A9 L Cells by Several Muscarinic Agonists[a]

ligand	% high	K_H (nM)	% low	K_L (μM)
carbachol	19 ± 3.8	56 ± 38	80 ± 3.8	8.4 ± 0.72
1a			93 ± 0.44	3.3 ± 0.92
2a			95 ± 1.2	0.57 ± 0.11
arecoline			100 ± 1.6	0.87 ± 0.25
4	29 ± 10	16 ± 8.0	71 ± 10	0.46 ± 0.072

[a] Data represent the mean (±sem) percentage of binding sites and K_i values for each site. K_i values were calculated using IC_{50} values obtained by nonlinear curve fitting, according to the best fit ($p < 0.05$) of the binding data to a one- or two-site model. The data are from three separate binding assays, each determined in triplicate.

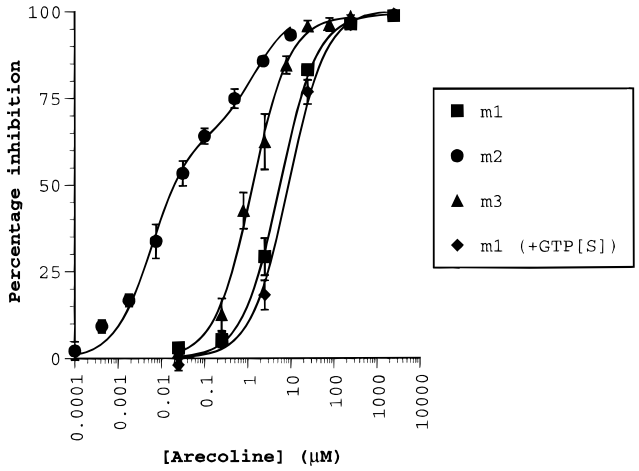

Figure 2. Inhibition of [^{3}H]-(*R*)-QNB binding to m1, m2, and m3 receptors expressed in A9 L cells by arecoline in the absence of GTP-γ-S (GTP[S]). Also shown is the inhibition of the binding [^{3}H]-(*R*)-QNB to m1 receptors by arecoline in presence of 300 μM GTP-γ-S. Data represent the mean (±sem) from three experiments, each performed in triplicate.

suggest the differences in agonist potencies between receptor subtypes may relate to the coupling of receptors to different G-proteins. The finding that each agonist bound with the highest affinity to m2 receptors suggests that it will be difficult to develop selective muscarinic

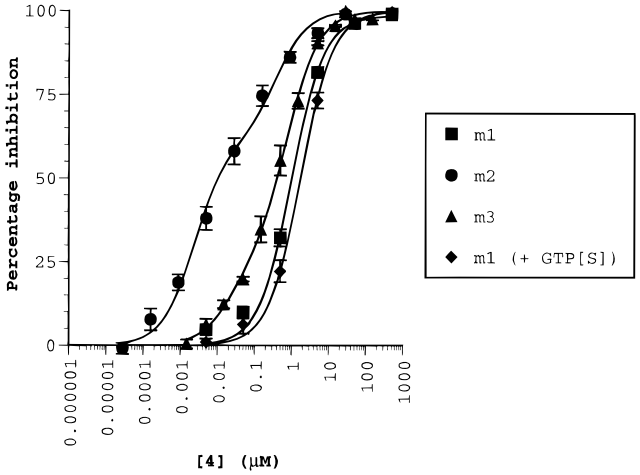

Figure 3. Inhibition of [^{3}H]-(*R*)-QNB binding to m1, m2, and m3 receptors expressed in A9 L cells by compound **4** in the absence of GTP-γ-S (GTP[S]). Also shown is the inhibition of the binding [^{3}H]-(*R*)-QNB to m1 receptors by **4** in presence of 300 μM GTP-γ-S. Data represent the mean (±sem) from three experiments, each performed in triplicate.

agonists solely on the basis of receptor affinity. Thus, future drug development efforts should focus on enhancing functional selectivity rather than increasing ligand potency. In addition, it will be important to examine agonist affinity for m4 and m5 receptors.

Functional Activity and Selectivity. Activity at m1 muscarinic receptors was examined using an A9 L cell line expressing human m1 receptors. Classical muscarinic agonists such as carbachol and oxotremorine-M, which contain a quaternary amine, stimulated PI metabolism in A9 L cells, while tertiary amines (e.g., oxotremorine, arecoline, and arecedaine propargyl ester (**3b**)) displayed lower efficacy at m1 receptors (see Table 6). Both **1a** and **2a** stimulated PI metabolism to maximal levels comparable to that of carbachol as shown in Figure 6A. Compound **1a** was much less potent than carbachol, while **2a** was even more potent. As shown in Figure 6C and Table 6, **1f** stimulated m1 receptors to a maximal level comparable to carbachol,

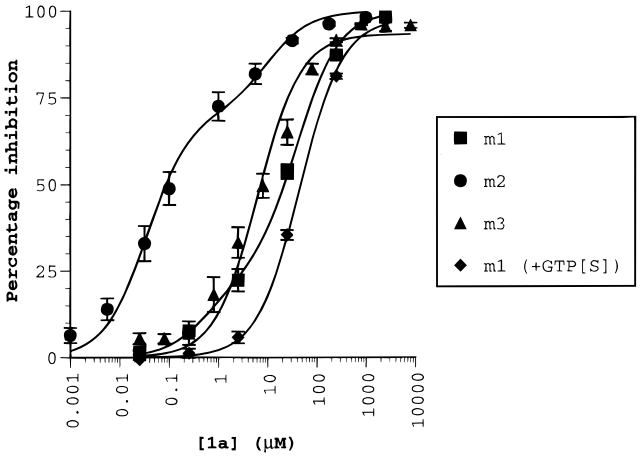

Figure 4. Inhibition of [^{3}H]-(*R*)-QNB binding to m1, m2, and m3 receptors expressed in A9 L cells by compound **1a** in the absence of GTP-γ-S (GTP[S]). Also shown is the inhibition of the binding [^{3}H]-(*R*)-QNB to m1 receptors by **1a** in presence of 300 μM GTP-γ-S. Data represent the mean (±sem) from three experiments, each performed in triplicate.

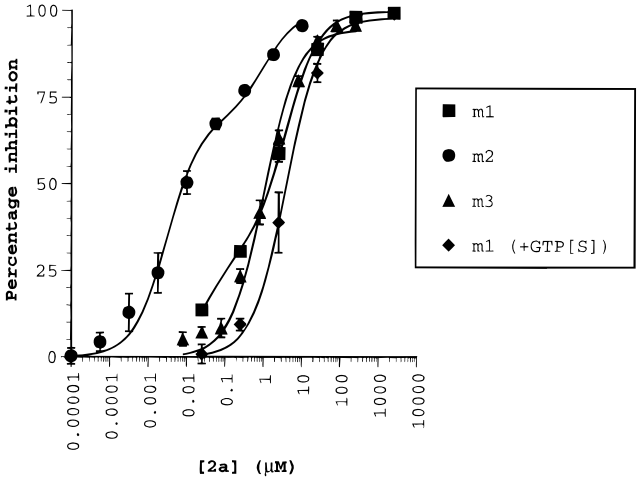

Figure 5. Inhibition of [^{3}H]-(*R*)-QNB binding to m1, m2, and m3 receptors expressed in A9 L cells by compound **2a** in the absence of GTP-γ-S (GTP[S]). Also shown is the inhibition of the binding [^{3}H]-(*R*)-QNB to m1 receptors by **2a** in presence of 300 μM GTP-γ-S. Data represent the mean (±sem) from three experiments, each performed in triplicate.

while **1b** and **2b** displayed intermediate activity. Compound **1f** was approximately as potent as carbachol in stimulating m1 receptors. Other tetrahydropyrimidine derivatives, including **1g**, **1h**, and **2k**, also exhibited high efficacy at m1 receptors, although the butynyl ester (**1h**) and oxadiazole (**2f**) exhibited much lower potency.

Functional muscarinic receptor selectivity was examined using the A9 L cell line expressing a high level of m3 receptors (see Figure 6B,D and Table 7). Carbachol stimulated m3 receptors coupled to PI metabolism in A9 L cells, although the maximum level of stimulation was roughly half that found for m1 receptors expressed in the same cell line. Overall, **1f**, **1b**, **2b**, and **7b** displayed markedly lower efficacy than carbachol (see Figure 6D), as did xanomeline in one experiment. Agonist potencies at m3 receptors were comparable to those found for m1 receptors.

On the basis of the relative activity and selectivity of compounds for m1 receptors, a few compounds were evaluated for activity at m2 receptors coupled to the inhibition of adenylyl cyclase activity in A9 L cells (see Table 8). Carbachol, xanomeline, and **2a** inhibited forskolin-stimulated adenylyl cyclase activity by greater than 20%. The propargyl esters **1f** and **7b** were much less effective in reversing the effects of forskolin on cAMP levels.

The availability of cell lines stably expressing individual muscarinic receptor subtypes provides useful tools for exploring agonist activity and functional selectivity. Depending upon the level of receptor expression, however, agonist responses in cell lines may not reflect accurately the response observed in brain tissue,[41] the relevant tissue for developing muscarinic agonists to treat Alzheimer's disease. The low activity of arecoline in A9 L cells expressing either m1 or m3 receptors is consistent with data obtained for PI metabolism in the CNS[20,42−44] and cAMP formation in A9 L cells expressing m1 receptors.[45] Furthermore, the effects of carbachol and arecoline on cAMP accumulation observed in A9 L cells are comparable to those observed previously for brain tissue.[19,46] Overall, these data suggest that A9 L cells provide a suitable paradigm for evaluating muscarinic receptor agonist activity and selectivity, although further studies are necessary to determine the level of agonist activity and subtype selectivity of the responses in brain.

The activity of 1,4,5,6-tetrahydropyrimidine derivatives in A9 L cells expressing m1 receptors was consistent with responses observed previously at muscarinic receptors coupled to PI metabolism in the rat central nervous system.[29,30] Moreover, the agonist activity of compounds **1a**, **1f**, and **2a** at m1 receptors suggests that they should be considered fully efficacious muscarinic agonists (class A compounds according to the classification proposed by Fisher).[20,43] In rat hippocampal slices, however, the maximal level of PI metabolism produced by **1a** is only a fraction of that produced by the corresponding oxadiazole derivative (**2a**).[29,30] In those studies, the M_1 antagonist pirenzepine blocked the PI response elicited by low doses of either **1a** or **2a**. The M_2- and M_3-selective antagonists, AF-DX 116 and *p*-F-hexahydrosiladifenidol, respectively, were less potent in blocking agonist activity. On the basis of the comparable efficacy displayed in the present studies, the higher efficacy of **2a** in rat hippocampus may be due to activation of other muscarinic receptor subtypes.

Taken together, the assays of functional activity at and selectivity for muscarinic receptor subtypes indicated a few agonists with high activity and functional selectivity for m1 muscarinic receptors. In particular, compounds **1b**, **1f**, and **2b** exhibited functional selectivity for m1 receptors, with reasonable potency and efficacy at m1 receptors, and lower efficacy at m2 and/or m3 receptors. It should be noted that these compounds compared favorably with xanomeline, an m1 agonist currently under clinical investigation for the treatment of Alzheimer's disease. In particular, compounds **1b**, **1f**, and **2b** showed higher efficacy than xanomeline at m1 receptors expressed in A9 L cells.

Molecular Modeling. The relative energies and molecular volumes for the different conformations of **1a** and arecoline are indicated in Table 9 and Figure 7A,B. Molecular mechanics calculations using the modified MM2 force field[47] revealed three minimum energy conformations for arecoline, yet six unique conformers for **1a**. Similar results were obtained using the modified AMBER force field,[48] except that two and five conformations were observed for arecoline and compound **1a**,

Table 6. Potency and Efficacy for a Series of Ligands at m1 Muscarinic Receptors Expressed in A9 L Cells[a]

ligand	R group	EC_{50} (μM)	S_{max} (%)
carbachol		40 ± 15	630 ± 110
oxo-M		0.70 ± 0.30	380 ± 36
oxotremorine		0.27 ± 0.19	120 ± 27
pilocarpine		6.9 ± 1.4	150 ± 18
arecoline		27 ± 2.7	180 ± 20
3b		0.22 ± 0.07	140 ± 30
4		12 ± 6.4	98 ± 29
xanomeline		5.7 ± 2.3	180 ± 24
1a	methyl	200 ± 51	660 ± 110
1b	ethyl	44 ± 5.2	330 ± 75
1f	propargyl	33 ± 6.6	590 ± 92
1g	2-butynyl	50 ± 6.5	430 ± 20
1h	butynyl	560 ± 420	340 ± 56
1l	*trans*-3-methyl-2-penten-4-ynyl		
1m	*cis*-3-methyl-2-penten-4-ynyl	80 ± 57	58 ± 1.1
2a	methyl	5.4 ± 1.4	640 ± 150
2b	ethyl	12 ± 1.2	330 ± 52
2f	butynyl	110 ± 14	360 ± 39
2k	(methylthio)methyl	14 ± 1.5	210 ± 21
7a	methyl	41 ± 5.1	400 ± 56
7b	ethyl	116 ± 3.5	220 ± 20
8a	methyl	160 ± 73	210 ± 31
8b	ethyl	300 ± 160	190 ± 10

[a] Data represent the mean (±sem) from one to three experiments, each performed in duplicate.

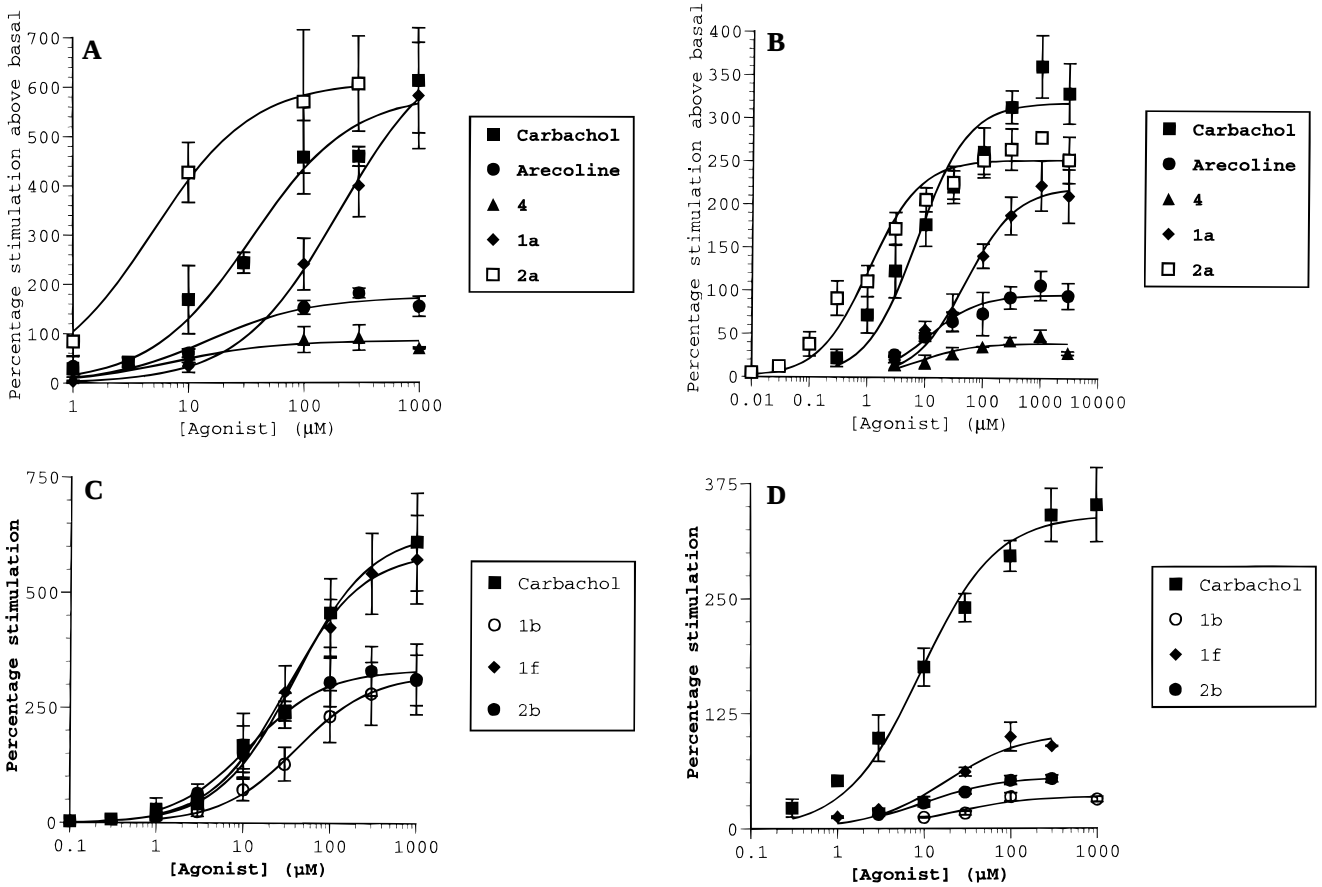

Figure 6. (A) Stimulation of PI metabolism by carbachol, arecoline, **1a**, **2a**, and **4** in A9 L cells expressing m1 muscarinic receptors. (B) Stimulation of PI metabolism by carbachol, arecoline, **1a**, **2a**, and **4** in A9 L cells expressing m3 muscarinic receptors. (C) Stimulation of PI metabolism by carbachol, **1b**, **1f**, and **2b** in A9 L cells expressing m1 muscarinic receptors. (D) Stimulation of PI metabolism by carbachol, **1b**, **1f**, and **2b** in A9 L cells expressing m3 muscarinic receptors. Data represent the mean stimulation above basal levels from at least three assays for each concentration of ligand, each performed in triplicate. The curves were generated by iterative fit to the equation: $Y = (S_{max}x)/(x + EC_{50})$ from the data shown in the figure.

respectively, within the 21 kJ/mol energy interval above the global minimum. The double bond in the 1,2,5,6-tetrahydropyridine system may limit the number of stable conformations in the arecoline series of compounds, while the 1,4,5,6-tetrahydropyrimidine system permits more energy minima upon rotation around the carbon−carbon bond between the tetrahydropyrimidine ring and the ester or 1,2,4-oxadiazole moiety. In addition to conformational constraints, the *N*-methyl group in arecoline and **4** may contribute to the relatively low

Table 7. Potency and Efficacy for a Series of Muscarinic Agonists at m3 Muscarinic Receptors Expressed in A9 L Cells[a]

ligand	EC_{50} (μM)	S_{max} (%)
carbachol	9.9 ± 2.6	350 ± 16
aceclidine	10 ± 3.7	130 ± 8.6
xanomeline	11	50
1a	50 ± 9.0	220 ± 8.4
1b	17 ± 12	32 ± 5.3
1f	18 ± 6.6	100 ± 9.7
2a	1.1 ± 0.24	250 ± 8.3
2b	10 ± 1.5	56 ± 1.9
2h	11 ± 2.4	110 ± 5.5
2k	5.8 ± 2.9	98 ± 13
arecoline	12 ± 3.3	96 ± 4.8
4	2.8 ± 1.7	40 ± 4.0
7a	14 ± 2.9	140 ± 5.9
7b	12 ± 9.1	31 ± 5.2

[a] Data represent the mean (±sem) from one to three experiments, each performed in duplicate.

Table 8. Inhibition of Forskolin-Induced cAMP Production in A9 L Cells Expressing m2 Receptors[a]

ligand	IC_{50} (μM)	% inhibn
carbachol	0.10 ± 0.06	24 ± 3.0
xanomeline	7.0 ± 3.0	44 ± 5.0
1a	1.6 ± 1.7	13 ± 6.0
1f	0.78 ± 0.55	12 ± 3.0
2a	0.11 ± 0.010	21 ± 7.0
arecoline	1.2 ± 0.51	12 ± 3.0
4	1.2 ± 0.59	16 ± 2.0
7b	0.44	10

[a] Data represent the mean (±sem) IC_{50} values and percentage inhibition as determined from one to four separate experiments for each ligand, each performed in duplicate.

Table 9. Relative Energy Values and Molecular Volumes for Different Conformations of **1a** and Arecoline[a]

ligand	rel energy (kJ/mol)	mol vol (Å^3)
1a i	0	131.9
1a ii	8.53	130.9
1a iii	9.37	131.4
1a iv	10.5	132.0
1a v	14.6	130.8
1a vi	16.1	131.5
arecoline i	0	152.8
arecoline ii	12.5	152.3
arecoline iii	12.6	152.3

[a] Data were obtained for the protonated species of each ligand.

efficacy of the 1,2,5,6-tetrahydropyridine derivatives. The methyl group may prevent close interaction between the negative Asp105 and the protonated site of the ligand (see below). The arecoline conformers had a larger molecular volume than the conformers of **1a**, due primarily to the additional methyl group on arecoline (see Table 9). The methyl group, however, may be advantageous in the interaction with residues in the binding pocket other than Asp105.[49]

Color codes of partial atomic charges, calculated by molecular orbital methods and taken at the van der Waals surface, indicated similar patterns over the ester as well as oxadiazole groups for both the tetrahydropyridine and tetrahydropyrimidine systems as seen in Figure 7C. The positive charge region was more extended for the 1,4,5,6-tetrahydropyrimidine ring system as compared to the 1,2,5,6-tetrahydropyridine ring. The charge distribution of the amidine system may confer higher agonist activity, since both **1a** and **2a** display higher efficacy than their 1,2,5,6-tetrahydropyridine analogs. The relative merits of the conformationally flexible system, the increase of molecular volume, and the amidine-like charge distribution in producing higher muscarinic agonist activity can be addressed by synthesizing derivatives combining these molecular features.

The interaction of muscarinic agonists with the m1 receptor was examined through a series of docking studies using the nine amino acid model of the m1 receptor binding site developed by Nordvall and Hacksell.[50] Molecular modeling studies, in combination with site-directed mutagenesis studies, have identified several amino acids believed to be involved in ligand binding to muscarinic receptors. In particular, an aspartate residue (Asp105 for the m1 receptor) appears critical for interaction of the onium head group of acetylcholine and carbachol with muscarinic receptor subtypes. In addition, site-directed mutagenesis studies[51,52] and molecular modeling approaches[50,53] have implicated threonine, tyrosine, and asparagine residues as potential hydrogen bond donors for the ester moiety of muscarinic ligands. As shown in Figure 8 and Table 10, docking studies (using the program Sybyl)[54] revealed hydrogen bond interactions between simple esters (such as arecoline and compound **1a**) and the Asp105 and the Thr192 residues, yet not with the Asn382 side chain. In contrast, both 1,2,4-oxadiazole derivatives (**2a** and **4**) could interact via a three-point contact with the aspartate, threonine, and asparagine residues.

An important finding from the present studies is that isosteric replacement of an ester with the 1,2,4-oxadiazole group increases the affinity for m1 receptors, without dramatically affecting coupling to second messenger systems. The data suggest that the oxadiazole moiety does not enhance efficacy at m1 receptors, but may be useful in increasing agonist potency for m1 receptors. The utility of the 1,2,4-oxadiazole moiety in enhancing ligand potency relative to simple esters could thus be explained by an additional interaction of the oxadiazole ring with the asparagine residue. This concept of hydrogen bonding to Thr192 and Asn382 also fits with the finding of low potencies and efficacies for ether and oxime derivatives. The oxygen is in the wrong position for hydrogen bonding in the ether derivatives, and its charge is reduced in oximes by the nitrogen, thereby reducing the ability to hydrogen bond to Thr192. This hypothesis is particularly attractive since recent site-directed mutagenesis studies indicate that the asparagine moiety is not as important for the binding and activity of small muscarinic agonists (e.g., acetylcholine, carbachol, and pilocarpine) to m3 muscarinic receptors, yet is critical for the high-affinity interaction of larger ligands such as *N*-methylscopolamine.[52] Additional studies of the binding of these ligands to mutant receptors are necessary to verify the potential hydrogen-bonding interaction of the oxadiazole moiety with the asparagine residue of muscarinic receptor subtypes.

Taken together, experimental data and molecular-modeling results suggest that the tetrahydropyrimidine moiety is an important determinant for agonist activity at m1 receptors. Three structural factors may contribute to agonist efficacy at m1 muscarinic receptors: conformational flexibility, molecular volume, and the charge distribution of the amidine system. By the same analysis, the 1,4,5,6-tetrahydropyrimidine system seems to be a better starting point than the 1,2,5,6-tetrahydropyridine system in the development of efficacious ligands.

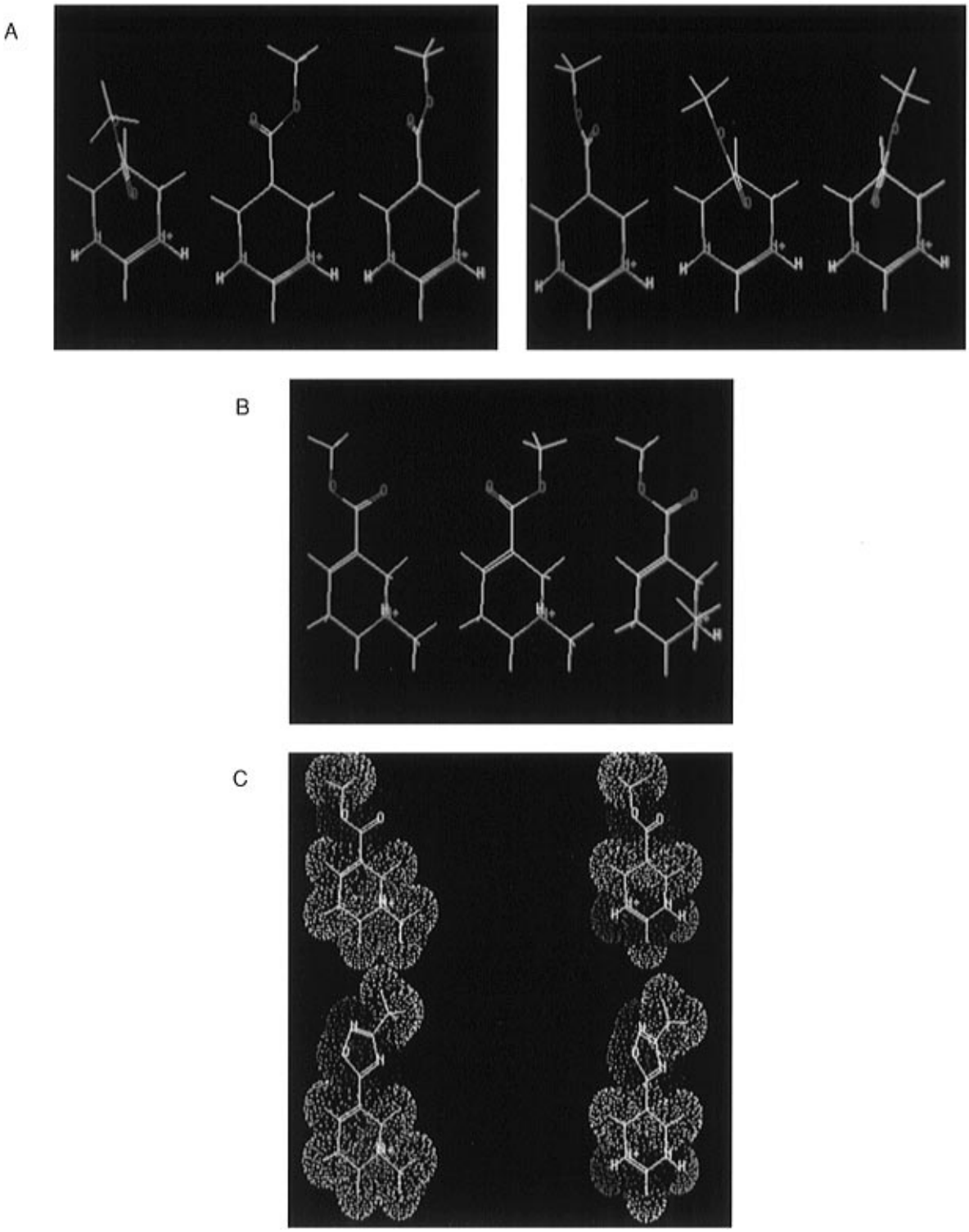

Figure 7. (A) Six minimum energy conformations of **1a** as determined from molecular mechanics calculations using the MM2 force field and the multiconformer submode as implemented in the program MacroModel (v 3.0). (B) Three minimum energy conformations of arecoline as determined using similar methods. (C) Color-coded van der Waal's surfaces for the lowest energy conformations of arecoline, **1a**, **2a**, and **4**. Data were generated from semiempirical MNDO partial atomic charges. Charges greater than +0.25 are indicated in blue, charges close to zero are in white, and negative charges less than −0.25 are in red.

Summary

The results of the present study provide new information regarding the activity and selectivity of the tetrahydropyrimidine derivatives. In addition, important functional features were identified for agonist potency, activity, and selectivity for muscarinic receptor subtypes. Perhaps of greatest importance is that the methyl (**1a**) and propargyl (**1f**) esters and the methyl-1,2,4-oxadiazole (**2a**) tetrahydropyrimidine derivatives displayed high efficacy at m1 muscarinic receptors coupled to PI metabolism, confirming previous observations in brain tissue.[29,30] In addition, the data revealed an important contribution of the 1,2,4-oxadiazole moiety in enhancing potency (yet not efficacy). Preliminary modeling studies suggested that the enhanced potency could be due to an additional interaction of the oxadiazole ring with the asparagine residue believed to be involved in ligand binding to muscarinic receptors.[50,53] Finally, compounds **1b**, **1f**, **2b**, and **7b** displayed functional selectivity for m1 muscarinic receptors as indi-

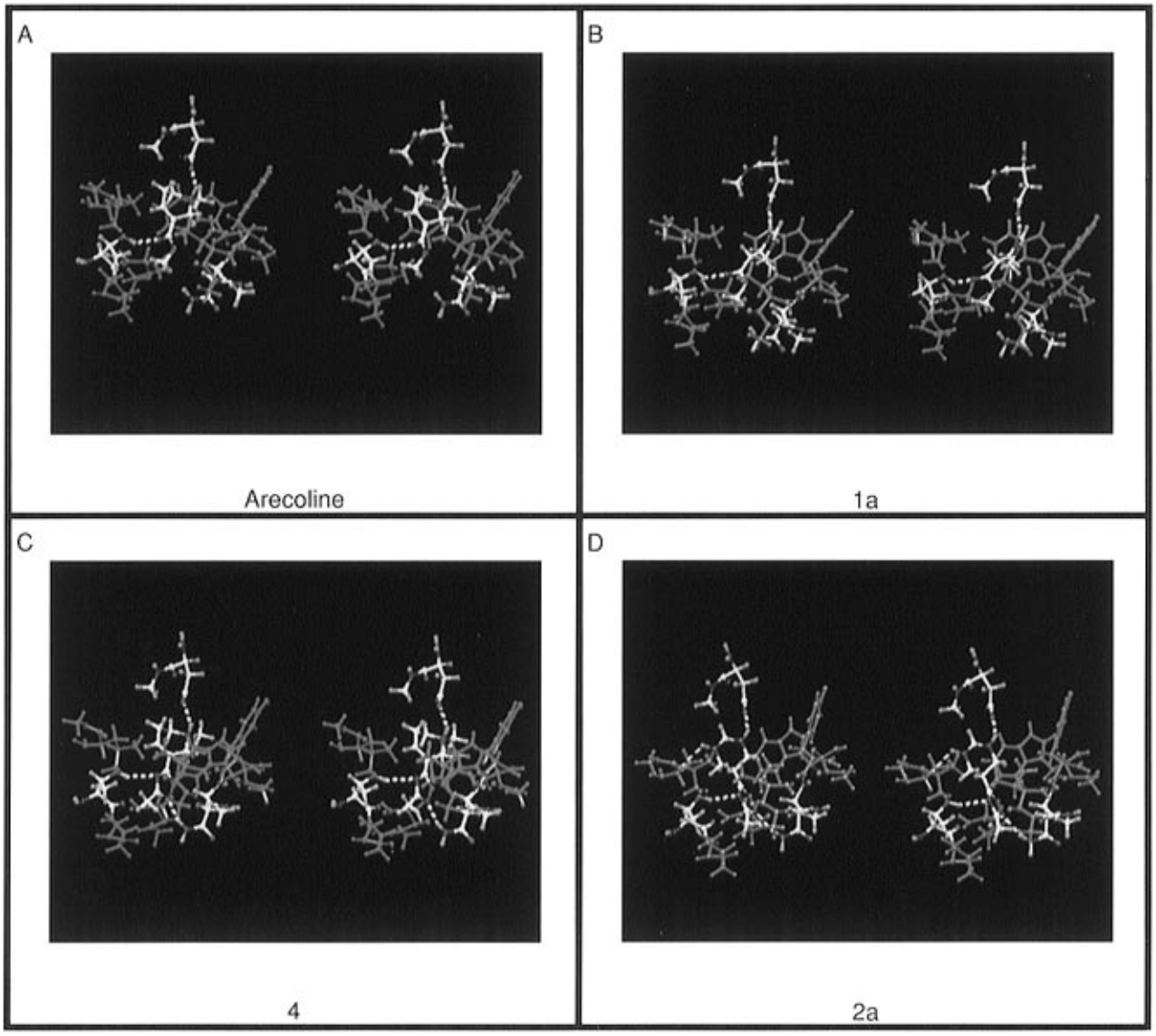

Figure 8. Stereoviews of some binding modes obtained by docking of muscarinic ligands to a nine amino acid model of the m1 muscarinic receptor.[50] The aspartate (top), threonine (left), and asparagine (right) residues are coded by atom type, as are the individual ligands, with carbon as white; hydrogen, blue; oxygen, red; and nitrogen, blue. Potential hydrogen bond interactions are shown by dashed yellow lines. (A) Docking of arecoline to the m1 receptor model revealing two hydrogen bond interactions. (B) Docking of **1a** to the m1 receptor model revealing two hydrogen bond interactions. (C) Docking of **4** to the m1 receptor model revealing three hydrogen bond interactions. (D) Docking of **2a** to the m1 receptor model revealing four hydrogen bond interactions, including a hydrogen bond to the carbonyl oxygen of the polypeptide backbone.

cated by full agonist activity at m1 receptors and lower activity at m3 receptors. Compounds **1f** and **7b** also displayed relatively low activity at m2 receptors. These compounds warrant further evaluation as selective muscarinic agonists for the treatment of Alzheimer's disease.

Experimental Section

Synthetic Chemistry. Compounds were synthesized utilizing reagent grade chemicals commercially available from Aldrich Chemical Co. and Fisher Scientific without further purification. Compounds **1a**, **1b**, **1f**, **2a**, **2b**, **4**, **5a**, **7a**, **7b**, **8a**, **8b**, and xanomeline were synthesized according to literature procedures.[29−31,34,55] Note that both **7a** and **7b** were synthesized as racemates. Nuclear magnetic resonance spectra were obtained on a Bruker ACF 300 MHz NMR in deuteriochloroform, deuteriomethanol, or deuterium oxide, using either TMS or TSP as an internal standard. Mass spectra were performed on a Hewlett-Packard 5890 spectrometer. TLC was performed on Kodak Chromatogram sheet 13181 silica gel with a fluorescent indicator (F254). Melting points were taken on an Electrothermal digital melting point apparatus and are presented uncorrected. Elemental analyses were performed by M-H-W Laboratories, Phoenix, AZ, and by the Chemical Department of the University of Toledo. Analytical results indicated by elemental symbols were within ±0.4% of the theoretical values, except where noted for compounds **1e** and **6c**, for which carbon values were off by 0.5 and 0.8%, respectively.

5-(2-Methylbutyloxycarbonyl)-1,4,5,6-tetrahydropyrimidine Hydrochloride (1d). 1,4,5,6-Tetrahydropyrimidine-5-carboxylic acid hydrochloride[29] (0.5 g, 3 mmol) was dissolved in anhydrous 3-methyl-1-butanol (50 mL), and thionyl chloride (0.2 mL, 3 mmol) was added dropwise with stirring at room temperature. The solution was refluxed over a period of 24 h and then evaporated to dryness *in vacuo*. The resulting crude residue was recrystallized from methanol−diethyl ether to give 0.4 g (89%) of the orange liquid of 5-(2-methylbutyloxycarbonyl)-1,4,5,6-tetrahydropyrimidine (**1d**) as the hydrochloride salt: ^{1}H NMR (D_2O) δ 0.9 (d, 6H), 1.2 (q, 2H), 1.5 (m, 1H), 3.1 (m, 1H), 3.5 (d, 4H), 3.9 (t, 2H), 7.9 (s, 1H). Anal. ($C_{10}H_{19}N_2O_2$-Cl) C, H, N.

***(R,S)*-5-(3-Methylbutyloxycarbonyl)-1,4,5,6-tetrahydropyrimidine Hydrochloride (1e).** 1,4,5,6-Tetrahydropyrimidine-5-carboxylic acid hydrochloride[29] (0.5 g, 3 mmol) was

Table 10. Relative Energies and Hydrogen Bonding Interactions of Four Ligands with a Theoretical Model of the m1 Muscarinic Receptor[a]

ligand	docking orientation	rel energy (kJ/mol)	H-bond Asp105	H-bond Thr192	H-bond Asn382
1a i	0	17.3	x	x	
	90	34.4		x	
	180	0.00	xx		
	270	18.1	x	x	
1a ii	0	8.87	x	x	
	90	15.3	x		
	180	17.0	x		
	270	7.26	x	x	
1a iii	0	20.0	x	x	
	90	35.3			
	180	9.25	x	x	
	270	20.2	xx	x	
1a iv	0	23.2	x	x	
	90	31.5			
	180	41.9			
	270	27.0	x	x	
1a v	0	16.3	x		
	90	6.54	x		
	180	32.9			
	270	14.1	x	x	
2a i	0	8.69	xx		
	90	3.12	x		x
	180	20.4	x	x	x
	270	9.05	x	x	
2a ii	0	0.00	x	x	
	90	3.09	x	xx	
	180	28.4	xx		
	270	17.1	xx		
2a iii	0	17.8	x		x
	90	30.2	x	x	
	180	28.4	x		
	270	4.2	x		x
2a iv	0	2.64	x	x	
	90	6.76	x		
	180	25.8			
	270	7.76	xx	x	
arecoline i	0	13.6	x	x	
	90	27.4		x	
	180	22.4	x	x	
	270	30.6		x	
arecoline ii	0	6.70		x	
	90	0.00	xx		
	180	5.30	xx		
	270	41.6			x
4 i	0	22.0	x	x	x
	90	37.5		x	x
	180	45.3		x	
	270	41.2		x	
4 ii	0	21.0	x	x	
	90	0.00	xx	x	
	180	36.5	x		
	270	25.2	x		x
7b i	0	>100			
	90	51.8	x	x	
	180	26.6	x	x	
	270	0.0	x		x
7b ii	0	40.5	x		
	90	61.2	x		
	180	39.9			
	270	23.1	x	x	
7b iii	0	20.4	x	x	
	90	6.64	x	x	x
	180	33.7	x		
	270	50.5	x	x	
7b iv	0	15.0	x	x	
	90	39.5	x	x	
	180	56.4	x	x	
	270	8.06	x		

[a] Data were obtained for the protonated species of each ligand. Hydrogen bond interactions (x) were defined by H−O or H−N distances less than 3.000 Å. Two hydrogen bonds to the same residue are indicated as xx.

esterified in racemic 2-methyl-1-butanol (50 mL) by a method virtually identical to that used for **1d**. The crude product was recrystallized from ethanol−diethyl ether to give 0.4 g (90%) of a viscous liquid of (*R,S*)-5-(2-methylbutyloxycarbonyl)-**1**,4,5,6-tetrahydropyrimidine (**1e**) as the hydrochloride salt: ^{1}H NMR (D_2O) δ 0.8 (t, 3H), 0.9 (s, 3H), 1.0 (m, 1H), 1.3 (m, 2H), 3.09 (m, 1H), 3.55 (d, 4H), 4.0 (m, 2H), 7.9 (s, 1H). Anal. ($C_{10}H_{19}N_2O_2Cl$) H, N; C: calcd, 51.2; found, 50.6.

5-(2-Butynyloxycarbonyl)-1,4,5,6-tetrahydropyrimidine Hydrochloride (1g). 1,4,5,6-Tetrahydropyrimidine-5-carboxylic acid chloride[31] (0.4 g, 2.2 mmol) was esterified in 2-butyn-1-ol (20 mL), employing a method virtually identical to that used for **1l**. The crude residue obtained was recrystallized from 2-propanol−diethyl ether to give off-white crystals (0.3 g, 61%) of 5-(2-butynyloxycarbonyl)-1,4,5,6-tetrahydropyrimidine (**1g**) as the hydrochloride salt: mp 139−140 °C; ^{1}H NMR (D_2O) δ 1.5 (t, 3H), 3.1 (m, 1H), 3.5 (d, 4H), 3.9 (q, 2H), 7.9 (s, 1H). Anal. ($C_9H_{13}N_2O_2Cl$) C, H, N.

5-(Butynyloxycarbonyl)-1,4,5,6-tetrahydropyrimidine Hydrochloride (1h). 1,4,5,6-Tetrahydropyrimidine-5-carboxylic acid chloride[31] (2 g, 11 mmol) was esterified in 3-butyn-1-ol (10 mL), employing a method virtually identical to that used for **11**. Recrystallization of the residue from 2-propanol−diethyl ether yielded reddish-brown crystals (0.6 g, 80%) of 5-(butynyloxycarbonyl)-1,4,5,6-tetrahydropyrimidine (**1h**) as the hydrochloride salt (hygroscopic): ^{1}H NMR (D_2O) δ 2.1 (t, 1H), 2.4 (m, 2H), 3.1 (m, 1H), 3.5 (d, 4H), 4.1 (t, 2H), 7.8 (s, 1H). Anal. ($C_9H_{13}N_2O_2Cl$) C, H, N.

5-(3-Pentynyloxycarbonyl)-1,4,5,6-tetrahydropyrimidine Hydrochloride (1i). 1,4,5,6-Tetrahydropyrimidine-5-carboxylic acid chloride[31] (0.4 g, 2.2 mmol) was esterified in 2-pentyn-1-ol (20 mL), employing a method virtually identical to that used for **1l**. Recrystallization of the residue from 2-propanol−diethyl ether yielded off-white crystals (0.25 g, 68%) of 5-(3-pentynyloxycarbonyl)-1,4,5,6-tetrahydropyrimidine (**1i**) as the hydrochloride salt: mp 179−180 °C; ^{1}H NMR (D_2O) 1.9−1.7 (t, 3H), 3.1 (m, 1H), 3.3−3.2 (q, 2H), 3.4 (d, 4H), 4.0 (d, 2H) 7.9 (s, 1H). Anal. ($C_{10}H_{15}N_2O_2Cl$) C, H, N.

5-(2-Pentynyloxycarbonyl)-1,4,5,6-tetrahydropyrimidine (1j). 1,4,5,6-Tetrahydropyrimidine-5-carboxylic acid chloride[31] (0.4 g, 2.2 mmol) was esterified in 3-pentyn-1-ol (20 mL), employing a method virtually identical to that used for **1l**. Recrystallization of the residue from 2-propanol−diethyl ether yielded pale yellow crystals (0.25 g, 62%) of 5-(2-pentynyloxycarbonyl)-1,4,5,6-tetrahydropyrimidine (**1i**) as the hydrochloride salt: mp 158−159 °C; ^{1}H NMR (D_2O) δ 1.9 (s, 3H), 3.2 (m, 1H), 3.4−3.2 (t, 2H), 3.5 (d, 4H), 4.0 (d, 2H), 7.8 (s, 1H). Anal. ($C_{10}H_{15}N_2O_2Cl$) C, H, N.

5-(Pentynyloxycarbonyl)-1,4,5,6-tetrahydropyrimidine Hydrochloride (1k). 1,4,5,6-Tetrahydropyrimidine-5-carboxylic acid chloride[31] (0.4 g, 2.2 mmol) was esterified in 4-pentyn-1-ol (20 mL), employing a method virtually identical to that used for **1l**. Recrystallization of the residue from 2-propanol−diethyl ether yielded pale yellow crystals (0.25 g, 72%) of 5-(pentynyloxycarbonyl)-1,4,5,6-tetrahydropyrimidine (**1i**) as the hydrochloride salt: mp 156−157 °C; ^{1}H NMR (D_2O) δ 2.2 (t, 1H), 3.1 (m, 1H), 3.2 (m, 2H), 3.4 (m, 2H), 3.6 (d, 4H), 3.7 (d, 2H), 7.9 (s, 1H). Anal. ($C_{10}H_{15}N_2O_2Cl$) C, H, N.

***trans*-5-(3-Methyl-2-penten-4-ynyloxycarbonyl)-1,4,5,6-tetrahydropyrimidine Hydrochloride (1l).** 1,4,5,6-Tetrahydropyrimidine-5-carboxylic acid hydrochloride[29] (1 g, 6 mmol) was suspended in a solution of oxalyl chloride (1.5 mL, 17 mmol) in benzene (10 mL), heated with stirring under reflux for 2.5 h, and then evaporated to dryness *in vacuo* after cooling, to give an orange-yellow residue. The last traces of oxalyl chloride were removed by adding 10 mL of benzene to the residue, and then the residue was evaporated to dryness *in vacuo* to give a crude residue of 1,4,5,6-tetrahydropyrimidine-5-carboxylic acid chloride (1.6 g).[31] A mixture of the acid chloride (0.4 g, 2.2 mmol) and *trans*-3-methyl-2-penten-4-yn-1-ol (10 mL, excess) was stirred at room temperature overnight. The reaction mixture was taken up in water (100 mL), stirred at room temperature for 2 h, and filtered. The dark-brown residue obtained on removal of solvents *in vacuo* was recrystallized (ethanol−ether) to give yellow crystals (0.3 g, 64%) of *trans*-5-(3-methyl-2-penten-4-ynyloxycarbonyl)-1,4,5,6-tetrahydropyrimidine (**1l**) as the hydrochloride salt: mp 144−145 °C; ^{1}H NMR (D_2O) δ 1.8 (m, 3H), 3.09 (m, 1H), 3.44 (s,

1H), 3.50 (d, 4H), 4.18 (d, 2H), 5.9 (t, 1H), 7.80 (s, 1H). Anal. ($C_{11}H_{15}N_2O_2Cl$) C, H, N.

***cis*-5-(3-Methyl-2-penten-4-ynyloxycarbonyl)-1,4,5,6-tetrahydropyrimidine Hydrochloride (1m).** 1,4,5,6-Tetrahydropyrimidine-5-carboxylic acid chloride[31] (0.4 g, 2.2 mmol) was esterified in *cis*-3-methyl-2-penten-4-yn-1-ol (15 mL) by a method virtually identical to that employed to synthesize **1l**. The dark-brown crude residue was recrystallized from ethanol−diethyl ether to give a brown viscous oil (0.4 g, 67%) of *cis*-5-(3-methyl-2-penten-4-ynyloxycarbonyl)-1,4,5,6-tetrahydropyrimidine (**1m**) as the hydrochloride salt: ^{1}H NMR (D_2O) δ 1.8 (m, 3H), 3.09 (m, 1H), 3.46 (s, 1H), 3.50 (d, 4H), 4.15 (d, 2H), 5.8 (t, 1H), 7.90 (s, 1H). Anal. ($C_{11}H_{15}N_2O_2Cl$) C, H, N.

***cis*-5-(3-Penten-1-ynyloxycarbonyl)-1,4,5,6-tetrahydropyrimidine Hydrochloride (1n).** 1,4,5,6-Tetrahydropyrimidine-5-carboxylic acid chloride[31] (0.5 g, 3 mmol) was esterified in *cis*/*trans*-2-penten-4-yn-1-ol (5 g, 60 mmol) by a method virtually identical to that used to synthesize **1l**. Recrystallization of the residue from methanol−diethyl ether yielded beige crystals (0.3 g, 78%) of *cis*-5-(3-penten-1-ynyloxycarbonyl)-1,4,5,6-tetrahydropyrimidine (**1n**) as the hydrochloride salt: mp 180−181 °C; ^{1}H NMR (D_2O) δ 2.15 (s, 1H), 3.09 (m, 1H), 3.46 (s, 1H), 3.50 (d, 4H), 4.15 (d, 2H), 5.8 (t, 1H), 7.80 (s, 1H). Anal. ($C_{10}H_{13}N_2O_2Cl$) C, H, N.

5-(2-Methylbutenyloxycarbonyl)-1,4,5,6-tetrahydropyrimidine Hydrochloride (1o). 1,4,5,6-Tetrahydropyrimidine-5-carboxylic acid chloride[31] (0.5 g, 2.7 mmol) was esterified in 3-methyl-2-buten-1-ol (20 mL) by a method virtually identical to that used to synthesize **1l**. Recrystallization of the crude residue from ethanol−diethyl ether yielded a brown viscous oil (0.4 g, 59%) of 5-(2-methylbutenyloxycarbonyl)-1,4,5,6-tetrahydropyrimidine (**1o**) as the hydrochloride salt: ^{1}H NMR (D_2O) δ 0.9 (s, 6H), 1.5 (m, 1H), 3.1 (m, 1H), 3.5 (d, 4H), 3.9 (m, 2H), 7.8 (s, 1H). Anal. ($C_{10}H_{17}N_2O_2Cl$) C, H, N.

5-(3-Methylpropynyloxycarbonyl)-1,4,5,6-tetrahydropyrimidine Hydrochloride (1p). 1,4,5,6-Tetrahydropyrimidine-5-carboxylic acid chloride[31] (0.3 g, 1.6 mmol) was esterified in 3-methylbutyn-2-ol (15 mL), employing a method virtually identical to that used for **1l**. The residue was recrystallized from ethanol−ether to give a red viscous oil (0.2 g, 54%) of 5-(3-methylpropynyloxycarbonyl)-1,4,5,6-tetrahydropyrimidine (**1p**) as the hydrochloride salt: ^{1}H NMR (D_2O) δ 1.5 (s, 3H), 2.3 (d, 1H), 3.09 (m, 1H), 3.5 (d, 4H), 3.8 (d, 1H), 7.9 (s, 1H). Anal. ($C_9H_{13}N_2O_2Cl$) C, H, N.

5-(3,3-Dimethylpropynyloxycarbonyl)-1,4,5,6-tetrahydropyrimidine Hydrochloride (1q). 1,4,5,6-Tetrahydropyrimidine-5-carboxylic acid chloride[31] (0.2 g, 1.1 mmol) was esterified in 2-methyl-3-butyn-2-ol (20 mL) by a method virtually identical to that used to synthesize **1l**. Recrystallization of the residue from methanol−diethyl ether yielded a red viscous oil (90 mg, 52%) of 5-(3,3-dimethylpropynyloxycarbonyl)-1,4,5,6-tetrahydropyrimidine (**1q**) as the hydrochloride salt: ^{1}H NMR (D_2O) δ 1.4 (s, 6H), 2.5 (m, 1H), 3.1 (m, 1H), 3.5 (d, 4H), 7.8 (s, 1H). Anal. ($C_{10}H_{15}N_2O_2Cl$) C, H, N.

5-(Phenylpropynyloxycarbonyl)-1,4,5,6-tetrahydropyrimidine Hydrochloride (1r). 1,4,5,6-Tetrahydropyrimidine-5-carboxylic acid chloride[31] (1 g, 6 mmol) was esterified in 3-phenyl-2-propyn-1-ol (10 mL) by a method virtually identical to that used for **1l**. The first recrystallization from ethanol and THF gave beige crystals (50 mg), mp 158−159 °C. ^{1}H NMR taken in deuteriomethanol indicated this compound was an impurity. The filtrate from the first recrystallization was then evaporated to dryness *in vacuo* to give an orange-yellow viscous oily residue. The residue was recrystallized from methanol−diethyl ether and dry THF to give white crystals (0.4 g, 62%) of 5-(phenylpropynyloxycarbonyl)-1,4,5,6-tetrahydropyrimidine (**1r**) as the hydrochloride salt: mp 117−118 °C; ^{1}H NMR (CD_3OD) δ 3.2 (m, 1H), 3.6 (d, 4H), 4.9 (s, 2H), 7.3−7.5 (m, 5H), 7.9 (s, 1H). Anal. ($C_{14}H_{15}N_2O_2Cl$) C, H, N.

5-(Propenyloxycarbonyl)-1,4,5,6-tetrahydropyrimidine Hydrochloride (1s). A mixture of 1,4,5,6-tetrahydropyrimidine-5-carboxylic acid chloride (0.4 g, 2.2 mmol) and 2-propen-1-ol (15 mL) was stirred at room temperature for 24 h. The reaction mixture was then taken up in water (50 mL), stirred at room temperature for 1.5 h, and filtered. The residue obtained on removal of solvents *in vacuo* was recrystallized from 2-propanol and diethyl ether to give off-white crystals (0.3 g, 75%) of 5-(propenyloxycarbonyl)-1,4,5,6-tetrahydropyrimidine as the hydrochloride salt: mp 150−151 °C; ^{1}H NMR (D_2O) 3.1 (m, 1H), 3.5 (d, 4H), 3.8 (d, 2H), 5.1−5.2 (dd, 2H), 5.7−5.9 (m, 1H), 7.8 (s, 1H). Anal. ($C_8H_{13}N_2O_2Cl$) C, H, N.

1-(Triphenylmethyl)-5-(3-(2-methylbutyl)-1,2,4-oxadiazol-5-yl)-1,4,5,6-tetrahydropyrimidine. 1-(Triphenylmethyl)-5-(3-(2-methylbutyl)-1,2,4-oxadiazol-5-yl)-1,4,5,6-tetrahydropyrimidine was synthesized according to literature procedures.[30] Sodium hydride (60% dispersion in mineral oil, 104 mg, 2.6 mmol) and 4-methylpentamidoxime[32] (130 mg, 2.6 mmol) were suspended in dry THF (20 mL) in an oven-dried round-bottom flask under a nitrogen atmosphere at 0 °C. After 60 min of stirring, the ice bath was removed and the gray suspension refluxed for 60 min to give a white suspension. 1-(Triphenylmethyl)-5-(methyloxycarbonyl)-1,4,5,6-tetrahydropyrimidine[30] (1 g, 2.6 mmol) solution in dry THF (30 mL) was added all at once, and reflux continued for 18 h. The solvents were evaporated to dryness *in vacuo*, and the residue was taken up in water (20 mL). The aqueous suspension was extracted exhaustively with chloroform, and the organic fractions were dried ($MgSO_4$). The residue obtained after removal of solvents *in vacuo* was chromatographed (silica, chloroform−methanol, 9:1) to yield a yellow semisolid residue of the crude cyclized product (1.2 g, 37%, $R_f = 0.38$).

5-[3-(2-Isopropyl)-1,2,4-oxadiazol-5-yl]-1,4,5,6-tetrahydropyrimidine Trifluoroacetate (2c). 5-[3-(2-Isopropyl)-1,2,4-oxadiazol-5-yl]-1,4,5,6-tetrahydropyrimidine trifluoroacetate (**2c**) was prepared by a method virtually identical to that employed to synthesize **2e**, with the exception that 2-methylpropamidoxime[32] (266 mg, 2.6 mmol) was used. After formation of the desired trifluoroacetate salt, the residue was recrystallized from ethanol−diethyl ether to yield 100 mg (38%) of a viscous reddish oil: ^{1}H NMR (D_2O) δ 1.1 (d, 6H), 2.1 (m, 1H), 3.10 (m, 1H), 3.65 (d, 4H), 7.8 (s, 1H); MS *m*/*z* 194 (M^+ of free base). Anal. ($C_{11}H_{15}F_3N_4O_3$) C, H, N.

5-[3-(2-Methylpropyl)-1,2,4-oxadiazol-5-yl]-1,4,5,6-tetrahydropyrimidine Trifluoroacetate (2d). 5-[3-(2-Methylpropyl)-1,2,4-oxadiazol-5-yl]-1,4,5,6-tetrahydropyrimidine trifluoroacetate (**2d**) was prepared by a method virtually identical to that used for **2e**, with the exception that 3-methylpentamidoxime[32] (302 mg, 2.6 mmol) was used. After formation of the desired trifluoroacetate salt, the residue was recrystallized from ethanol−diethyl ether to yield 100 mg (39%) of a viscous reddish oil: ^{1}H NMR (D_2O) δ 0.9 (d, 6H), 2.0 (m, 1H), 2.50 (d, 2H), 3.10 (m, 1H), 3.70 (d, 4H), 7.9 (s, 1H); MS *m*/*z* 208 (M^+ of free base). Anal. ($C_{12}H_{17}F_3N_4O_3$) C, H, N.

5-[3-(2-Methylbutyl)-1,2,4-oxadiazol-5-yl]-1,4,5,6-tetrahydropyrimidine Trifluoroacetate (2e). 1-(Triphenylmethyl)-5-(3-(2-methylbutyl)-1,2,4-oxadiazol-5-yl)-1,4,5,6-tetrahydropyrimidine was dissolved in trifluoroacetic acid (5 mL) with stirring, and the resulting yellow solution was warmed gently overnight for 24 h. The resulting dark solution was evaporated to dryness *in vacuo*, and the yellow residue was triturated with hexane (6 × 10 mL). The hexane layers were decanted, and the residue was recrystallized (ethanol−ether) to yield a viscous oily product (0.1 g, 39%) of 5-[3-(2-methylbutyl)-1,2,4-oxadiazol-5-yl]-1,4,5,6-tetrahydropyrimidine (**2e**) as the trifluoroacetate salt: ^{1}H NMR (D_2O) δ 0.7 (d, 6H), 1.45 (q, 2H), 2.0 (m, 1H), 2.30 (t, 2H), 3.20 (m, 1H), 3.60 (d, 4H), 8.0 (s, 1H); MS *m*/*z* 338 (M^+ of free base). Anal. ($C_{13}H_{19}F_3N_4O$) C, H, N.

3-Butynyl-*p*-toluenesulfonate. 3-Butynyl-*p*-toluenesulfonate was prepared utilizing an extension of literature procedures.[33,56] Tosyl chloride (191 g, 0.7 mol) was dissolved in anhydrous ether (1 L) in a 2-L three-necked round-bottomed flask equipped with a thermometer, mechanical stirrer, and powder funnel. 3-Butyn-1-ol (35 g, 38 mL, 0.50 mol) was added, and the mixture was cooled to between −5 and −10 °C (bath with dry ice and acetone) with rapid stirring. Freshly powdered KOH (250 g) was added with vigorous stirring. The addition was initially at the rate of 5 g of KOH every 2 min, so as to maintain the temperature between 0 and 5 °C. Evolution of heat was considerable; hence efficient cooling was required. After adding the first 50 g of KOH, over 20 min,

the remainder was added over an additional 10 min (to neutralize excess tosyl chloride). The mixture was stirred for an additional 1 h while maintaining the temperature between 0 and 5 °C. After 1 h of stirring, the mixture was poured into 1.5 L of ice water, and the solid remaining in the flask was quickly hydrolyzed with the ice water and subsequently added to the bulk of the solution. After vigorous shaking, the layers were separated. The organic layer (ether layer) and two ethereal extracts were combined and dried over anhydrous magnesium sulfate overnight. The ether was evaporated to dryness *in vacuo* while keeping the temperature of the water bath below 80 °C. The desired 3-butynyl tosylate was obtained as an orange-yellow liquid in an overall yield of over 90%: ^{1}H NMR ($CDCl_3$) δ 7.8 (2H, d), 7.4 (2H, d), 4.10 (2H, t), 2.6 (2H, m), 2.45 (3H, s), 2.0 (1H, t).

4-Cyano-1-butyne. 4-Cyano-1-butyne was prepared from the corresponding 3-butynyl-*p*-toluenesulfonate, employing an extension of literature procedures.[33,56] Dry, powdered NaCN (3.6 g, 73 mmol, excess), was dissolved with stirring in DMSO (30 mL). 3-Butynyl-*p*-toluenesulfonate (5 g, 4.5 mmol) was added slowly because of the exothermic nature of the reaction, all in a three-necked 1-L round-bottomed flask equipped with a condenser, thermometer, and magnetic stirrer. After all of the additions, the mixture was gradually heated to 70 °C using a temperature-controlled water bath. The reaction mixture was occasionally cooled during the additions so as to maintain the temperature within the desired range. After an additional 30 min of stirring at 70 °C, the mixture was cooled to room temperature and then poured into 400 mL of saturated aqueous ammonium chloride to give a dark-brown mixture. The dark-brown mixture was extracted several times with ether. The ether extracts were washed with aqueous ammonium chloride (2 × 100 mL), and the extracts were dried (K_2CO_3). The ether was removed *in vacuo*, and the remaining liquid was distilled on a Widmer column to yield 4.1 g (89%) of off-white liquid product: bp 60−61 °C/10 mmHg (lit.[33] bp 60 °C/10 mmHg); ^{1}H NMR (CD_3OD) δ 2.4 (1H, t), 2.5 (2H, m), 2.6 (2H, t).

5-(3-(Butyn-1-yl)-1,2,4-oxadiazol-5-yl)-1,4,5,6-tetrahydropyrimidine Trifluoroacetate (2f). 5-(3-(Butyn-1-yl)-1,2,4-oxadiazol-5-yl)-1,4,5,6-tetrahydropyrimidine trifluoroacetate (**2f**) was prepared by a method virtually identical to that used for **2e**, with the exception that 4-pentynamidoxime[32] (292 mg, 2.6 mmol) was used. After formation of the desired trifluoroacetate salt, the residue was recrystallized from ethanol−diethyl ether to yield 120 mg (40%) of viscous reddish oil: ^{1}H NMR (D_2O) δ 2.25 (t, 1H), 2.5 (q, 2H), 2.6 (t, 2H), 3.10 (m, 1H), 3.50 (d, 4H), 7.8 (s, 1H); MS *m*/*z* 204 (M^+ of free base). Anal. ($C_{12}H_{13}F_3N_4O_3$) C, H, N.

5-(3-(Pentyn-1-yl)-1,2,4-oxadiazol-5-yl)-1,4,5,6-tetrahydropyrimidine Trifluoroacetate (2g). 5-(3-(Pentyn-1-yl)-1,2,4-oxadiazol-5-yl)-1,4,5,6-tetrahydropyrimidine trifluoroacetate (**2g**) was prepared by a method virtually identical to that used for **2e**, with the exception that 5-hexynamidoxime[32] (328 mg, 2.6 mmol) was used. After formation of the desired trifluoroacetate salt, the residue was recrystallized from methanol−diethyl ether to yield 55 mg (18%) of yellow oil: ^{1}H NMR (D_2O) δ 1.83 (2H, m), 2.18 (3H, m), 2.76 (2H, t), 3.75 (1H, m), 3.77 (4H, d), 8.02 (1H, s). Anal. ($C_{13}H_{14}F_3N_4O_3$) C, H, N.

(Methyloxy)ethamidoxime. Hydroxylamine hydrochloride (5g, 72 mmol) was suspended in methanol (60 mL in a 100 mL, three-neck, round-bottom flask fitted with a condenser and dropping funnel) under nitrogen and cooled to 0 °C with stirring. Sodium (1.66 g, 72 mmol) was added slowly with the temperature maintained at 0 °C. (Methyloxy)acetonitrile (5.12 g, 72 mmol) in methanol (10 mL) was added dropwise to the white suspension. The mixture was allowed to warm to room temperature overnight with stirring. The mixture was heated to 40 °C with stirring for 6 h, cooled to room temperature, and vacuum-filtered, and the filtrate was evaporated *in vacuo*. The semisolid residue was dissolved in ethanol and filtered to remove traces of remaining sodium chloride. The filtrate was evaporated to yield 3.85 g (51%) of a brown oil: ^{1}H NMR (DMSO) δ 3.28 (3H, s), 3.84 (2H, s).

5-(3-((Methyloxy)methyl)-1,2,4-oxadiazol-5-yl)-1,4,5,6-tetrahydropyrimidine Trifluoroacetate (2h). 5-(3-((Methyloxy)methyl)-1,2,4-oxadiazol-5-yl)-1,4,5,6-tetrahydropyrimidine trifluoroacetate (**2h**) was prepared by a method virtually identical to that used for **2e**, with the exception that (methyloxy)methamidoxime (271 mg, 2.6 mmol) was used. After formation of the desired trifluoroacetate salt, the residue was recrystallized from ethanol−diethyl ether to yield 370 mg (50%) of a brown oil: ^{1}H NMR (CD_3OD) δ 3.40 (3H, s), 3.80 (1H, m), 3.85 (4H, d), 4.54 (2H, s), 8.10 (1H, s). Anal. ($C_{10}H_{13}F_3N_4O_4$) C, H, N.

3-(Methyloxy)propamidoxime. 3-(Methyloxy)propamidoxime was synthesized in a manner virtually identical to that used for (methyloxy)acetamidoxime, except that 3-(methyloxy)-propionitrile (6.54 mL, 72 mmol) was used. The resulting filtrate was evaporated to yield 4.62 g (54%) of a green oil: ^{1}H NMR (DMSO) δ 2.21 (2H, t), 3.21 (3H, s) 3.47 (2H, t), 5.55 (2H, s).

5-(3-((Methyloxy)ethyl)-1,2,4-oxadiazol-5-yl)-1,4,5,6-tetrahydropyrimidine Trifluoroacetate (2i). 5-(3-((Methyloxy)ethyl)-1,2,4-oxadiazol-5-yl)-1,4,5,6-tetrahydropyrimidine trifluoroacetate (**2i**) was prepared by a method virtually identical to that used for **2e**, with the exception that (methyloxy)propamidoxime (307 mg, 2.6 mmol) was used. After formation of the desired trifluoroacetate salt, the residue was recrystallized from methanol−diethyl ether to yield 212 mg (43%) of a yellow oil: ^{1}H NMR (CD_3OD) δ 2.97 (2H, t, J = 6), 3.30 (3H, s), 3.75 (2H, t, J = 6), 3.80 (1H, m), 3.87 (4H, d), 8.11 (1H, s). Anal. ($C_{11}H_{14}F_3N_4O_4$) C, H, N.

(Ethyloxy)propamidoxime. (Ethyloxy)propamidoxime was synthesized in a manner virtually identical to that used for 3-(methyloxy)acetamidoxime, except that (ethyloxy)propionitrile (7.84 mL, 72 mmol) was used. The resulting filtrate was evaporated to yield 4.62 g (54%) of a yellow oil: ^{1}H NMR (DMSO) δ 1.03 (3H, t), 2.21 (2H, t) 3.35 (2H, q), 3.50 (2H, t), 6.01 (2H, s).

5-(3-((Ethyloxy)ethyl)-1,2,4-oxadiazol-5-yl)-1,4,5,6-tetrahydropyrimidine Trifluoroacetate (2j). 5-(3-((Ethyloxy-)ethyl)-1,2,4-oxadiazol-5-yl)-1,4,5,6-tetrahydropyrimidine trifluoroacetate (**2j**) was prepared by a method virtually identical to that used for **2e**, with the exception that (ethyloxy)-propamidoxime (344 mg, 2.6 mmol) was used. After formation of the desired trifluoroacetate salt, the residue was recrystallized from methanol−diethyl ether to yield 200 mg (57%) of a yellow oil: ^{1}H NMR (CD_3OD) δ 1.03 (3H, t), 2.87 (2H, t), 3.38 (2H, q), 3.74 (7H, m), 8.01 (1H, s). Anal. ($C_{12}H_{17}F_3N_4O_4$) C, H, N.

(Methylthio)methamidoxime. Hydroxylamine hydrochloride (5g, 72 mmol) was suspended in methanol (30 mL) under nitrogen and cooled to 0 °C with stirring. Sodium methoxide (3.89 g, 72 mmol) suspended in methanol was added slowly with the temperature maintained at 0 °C. (Methylthio)-acetonitrile (6.27 g, 72 mmol) in methanol (10 mL) was added dropwise to the white suspension. The mixture was allowed to warm to room temperature overnight with stirring. The mixture was heated to 40 °C with stirring for 6 h, cooled to room temperature, and vacuum-filtered, and the filtrate was evaporated *in vacuo*. The residue was dissolved in ethanol and filtered to remove traces of remaining sodium chloride. The filtrate was evaporated to yield 7.36 g (85%) of a green viscous oil: ^{1}H NMR (DMSO) δ 1.89 (3H, s), 2.89 (2H, s), 5.38 (2H, s), 8.24 (1H, b).

5-(3-((Methylthio)methyl)-1,2,4-oxadiazol-5-yl)-1,4,5,6-tetrahydropyrimidine Trifluoroacetate (2k). 5-(3-((Methylthio)methyl)-1,2,4-oxadiazol-5-yl)-1,4,5,6-tetrahydropyrimidine trifluoroacetate (**2k**) was prepared by a method virtually identical to that used for **2e**, with the exception that (methylthio)methamidoxime (480 mg, 3.99 mmol) was used. After formation of the desired trifluoroacetate salt, the residue was recrystallized from ethanol−diethyl ether to yield 381 mg (51%) of a brown crystalline solid (mp 89−91 °C): ^{1}H NMR (CD_3OD) δ 2.01 (3H, s), 3.70 (1H, m), 3.76 (4H, d), 4.77 (2H, s), 8.10 (1H, s). Anal. ($C_{12}H_{13}F_3N_4O_3$) C, H, N.

1,4,5,6-Tetrahydro-5-(propynyloxy)pyrimidine Hydrochloride (5b). 5-Hydroxy-1,4,5,6-tetrahydropyrimidine[35] (2.3 g, 23 mmol) was dissolved in absolute ethanol (50 mL). Propargyl chloride (1.7 g, 1.6 mL, 23 mmol) was added slowly via a syringe followed by potassium carbonate (3.1 g, 23 mmol), and the mixture was heated with stirring under reflux. After

2.5 h, the mixture was filtered, and the filtrate was evaporated to dryness *in vacuo* to given an orange-yellow residue. The hydrochloride salt was obtained by addition of 1 M HCl in ether to an ethanol solution of the residue, evaporation of solvents to dryness *in vacuo*, and recrystallization (ethanol−ether) to give yellow crystals (2 g, 79%) of 5-(propynyloxy)-1,4,5,6-tetrahydropyrimidine as the hydrochloride salt (hygroscopic): ^{1}H NMR (CD_3OD) δ 1.1 (1H, t), 3.1 (1H, m), 3.45 (4H, d), 4.2 (2H, d), 7.9 (1H, s). Anal. ($C_7H_{11}N_2OCl$) C, H, N.

1,4,5,6-Tetrahydropyrimidin-5-one Hydrochloride. To a suspension of pyridinium chlorochromate (23 g) in CH_2Cl_2 (800 mL) was added 5-hydroxy-1,4,5,6-tetrahydropyrimidine (9.8 g).[35] The resulting mixture was stirred at room temperature for 18 h, Celite was added, and the mixture was filtered. The filtrate was washed with $NaHCO_3$ solution (2 × 50 mL), and the aqueous layers were extracted with CH_2Cl_2 (3 × 100 mL). The combined organic layers were dried (Na_2SO_4) and the solvents evaporated *in vacuo* to give a residue, which was purified by flash chromatography (silica, 60% ether−hexane or EtOAc−petroleum ether, 3:7) to give the ketone as the free base. The hydrochloride salt was obtained by addition of 1 M HCl in ether to an ethanol solution of the residue; evaporation of solvents to dryness *in vacuo* gave a brown residue. The residue was discolorized and purified with activated charcoal and then recrystallized from ethanol−diethyl ether to give white crystals (6.5 g, 57%) of 1,4,5,6-tetrahydropyrimidin-5-one as the hydrochloride salt: ^{1}H NMR (CD_3OD) δ 3.5 (s, 4H), 7.9 (s, 1H).

Methyl-1,4,5,6-tetrahydropyrimidin-5-one Oxime Hydrochloride (6a). Methoxylamine hydrochloride (0.3 g, 3 mmol) was suspended in methanol (20 mL) under a nitrogen atmosphere and cooled to 0 °C. Sodium methoxide, 95% (0.2 g, 3 mmol) suspension in methanol (20 mL), was added slowly with stirring, and the mixture was allowed to stir for 11 h at 0 °C under anhydrous conditions to generate the free base. 1,4,5,6-Tetrahydropyrimidin-5-one (0.3 g, 3 mmol) solution in methanol (20 mL) was added dropwise over a period of 1 h. The reaction mixture was allowed to warm to room temperature, and stirring continued for 18 h. The solvents were evaporated *in vacuo* to give a brown residue. The hydrochloride salt was obtained by addition of 1 M HCl in ether to an ethanol solution of the residue. Evaporation of solvents to dryness *in vacuo* gave a brown residue. The residue was discolorized and purified with activated charcoal and then recrystallized from 2-propanol−diethyl ether to give gray crystals (0.2 g, 51%) of methyl-1,4,5,6-tetrahydropyrimidin-5-one oxime as the hydrochloride salt: mp 147−148 °C; ^{1}H NMR (CD_3OD) δ 3.5 (s, 4H), 3.72 (s, 3H), 7.9 (s, 1H). Anal. ($C_5H_{10}N_3OCl$) C, H, N.

Ethyl-1,4,5,6-tetrahydropyrimidin-5-one Oxime Hydrochloride (6b). Ethyl-1,4,5,6-tetrahydropyrimidin-5-one oxime hydrochloride (**6b**) was prepared by a method virtually identical to that employed to synthesize **6a**, with the exception that ethoxylamine hydrochloride (0.3 g, 3 mmol), sodium methoxide, 95% (0.2 g, 3 mmol), and 1,4,5,6-tetrahydropyrimidin-5-one (0.3 g, 3 mmol) were used. After formation of the hydrochloride salt, the residue was recrystallized from 2-propanol−diethyl ether to yield 0.4 g (54%) of white crystals: mp 160−162 °C; ^{1}H NMR (CD_3OD) δ 1.2 (t, 3H), 3.5 (s, 4H), 4.0 (q, 2H), 7.9 (s, 1H). Anal. ($C_6H_{12}N_3OCl$) C, H, N.

3-Phenyl-2-propyn-1-ol. 3-Phenyl-2-propyn-1-ol was prepared by utilizing an extension of a literature procedure.[33] Diethylamine, 98% (100 mL, dried over powdered KOH), Pd(PPh_3)$_4$ catalyst (0.5 g, 0.4 mmol), and CuI (0.5 g, 2.6 mmol) were placed in a 250 mL, three-necked, round-bottomed flask. Propargyl alcohol (11 g, 12 mL, 0.2 mol) was added, after which the temperature rose to 45 °C. Then a mixture of bromobenzene (47 g, 32 mL, 0.3 mol) in dry THF (30 mL) (previously cooled to 5−10 °C) was added portionwise over 30 min, while the temperature was maintained between 45 and 50 °C (by controlled addition of bromobenzene solution and occasional cooling or heating). After 10 min, salt formation began from the solution. The mixture was gently refluxed for another 1 h, allowed to cool, and filtered to remove insoluble residues. The residue (salt) was washed with dry THF, filtrates were combined, and then the mixture was concentrated *in vacuo* (at a bath temperature ~50 °C). The remaining liquid was taken up in 150 mL of an aqueous solution containing 30 g of NH_4Cl and extracted (50 mL × 10) with THF. The extracts were combined and concentrated *in vacuo*, and the remaining liquid was vacuum distilled to give a yellow liquid (4.0 g, 58%) of 3-phenyl-2-propyn-1-ol: bp 128−129 °C/10 mm; ^{1}H NMR (CD_3OD) δ 4.30 (s, 2H), 7.2 (m, 3H), 7.3 (m, 2H).

***N*-(Phenylpropynoxy)phthalimide.** *N*-(Phenylpropynoxy)phthalimide was synthesized from 3-phenyl-2-propyn-1-ol using an extension of previously reported procedure.[56] 3-Phenyl-2-propyn-1-ol (3.3 g, 25 mmol), *N*-hydroxyphthalimide (4 g, 25 mmol), and triphenylphosphine (6 g, 25 mmol) were dissolved in dry tetrahydrofuran (120 mL) and treated with diethyl azodicarboxylate (DEAD, 4.8 g, 27 mmol). The reaction mixture became dark red, and the color disappeared after a few minutes. A slight exothermic effect was observed on mixing of the reagents. The reaction vessel was glass-stoppered and then left at room temperature for 24 h. The residue obtained after evaporation of solvents to dryness *in vacuo* was chromatographed (silica, benzene/ether, 9:1) to give a yellow viscous residue (13 g, R_f = 0.77). Recrystallization of the residue from ethanol gave an orange viscous liquid (12.7 g, 90%) of pure *N*-(phenylpropynoxy)phthalimide: ^{1}H NMR ($CDCl_3$) δ 4.35 (s, 2H), 7.25 (m, 3H), 7.35 (m, 2H), 7.90 (s, 4H).

Phenylpropynoxylamine. Phenylpropynoxylamine was obtained through an hydrazinolysis reaction of *N*-(phenylpropynoxy)phthalimide according to literature procedures.[56] *N*-(Phenylpropynoxy)phthalimide (12.6 g, 45 mmol) and hydrazine hydrate (1.5 g, 45 mmol) were dissolved in ethanol and heated with stirring under reflux. After 1 h the reaction mixture was cooled and poured into a 3% sodium carbonate solution to dissolve the *N*-aminophthalimide. The resulting hydroxylamine was extracted (100 mL × 3) with ether, and the extracts were dried ($MgSO_4$). The dried extracts was adjusted to pH 5 with anhydrous ethereal hydrogen chloride (1 M ether−HCl). After evaporation of solvents to dryness *in vacuo*, the orange-yellow residue obtained was recrystallized from ethanol and ether. The supernatant ether layer was decanted, evaporated to dryness *in vacuo*, and then dried in a vacuum oven at ~50 °C for 2 h to give an orange-yellow solid (8.5 g, 82%) of phenylpropynoxylamine: ^{1}H NMR ($CDCl_3$) δ 4.110 (s, 2H), 5.30 (br s, 2H), 7.15 (m, 3H), 7.25 (m, 2H).

(Phenylpropynyl)-1,4,5,6-tetrahydropyrimidin-5-one Oxime Hydrochloride (6c). (Phenylpropynyl)-1,4,5,6-tetrahydropyrimidin-5-one oxime hydrochloride (**6c**) was prepared by a method virtually identical to that used for **6a**, with the exception that phenylpropynoxylamine (0.9 g, 4.9 mmol) and 1,4,5,6-tetrahydropyrimidin-5-one (0.5 g, 4.9 mmol) were used. After formation of the hydrochloride salt, the residue was recrystallized from 2-propanol−diethyl ether to yield 0.4 g (61%) of white crystals: mp 115−116 °C; ^{1}H NMR (CD_3OD) δ 3.45 (s, 4H), 4.30 (s, 2H), 7.3 (m, 3H), 7.4 (m, 2H), 7.9 (s, 1H); MS *m*/*z* 227 (M^+ of free base). Anal. ($C_{13}H_{14}N_3OCl$) H, N; C: calcd 59.2; found 60.0.

Materials. A9 L cells stably transfected with the m1, m2, or m3 muscarinic receptor genes were received as a generous gift from Dr. Mark Brann (University of Vermont). Eagle's minimum essential medium (EMEM), Dulbecco's modified Eagle's minimum essential medium (DMEM), and L-glutamine were purchased from Whittaker Bioproducts (Walkersville, MD). Fetal bovine serum, penicillin G, and streptomycin were obtained from Sigma (St. Louis, MO). The 0.2 μm filterware (Nalge, Rochester, NY), plastic scrapers, and tissue culture flasks were from VWR Scientific.

[^{3}H]-(*R*)-Quinuclidinyl benzilate ([^{3}H]-(*R*)-QNB; 44.9 Ci/mmol) was obtained from Du Pont (Wilmington, DE). [^{3}H]-*myo*-Inositol was obtained from New England Nuclear (Boston, MA) with a specific activity of 12.3−20.0 Ci/mmol. The cAMP assay kit (cAMP [^{125}I] assay system code RPA 509) was purchased from Amersham. Carbamylcholine chloride (carbachol) was obtained from Aldrich (Milwaukee, WI). Arecoline hydrobromide, atropine sulfate, oxotremorine, and 4-(2-hydroxyethyl)-1-piperazineethanesulfonic acid (HEPES) were obtained from Sigma. Arecedaine propargyl ester was purchased from Research Biochemicals Incorporated. $MgCl_2$ was obtained from Fisher Scientific. CytoScint was purchased from ICN Biomedicals, Inc. (Irvine, CA).

Receptor Binding in Rat Brain. Binding to muscarinic receptors was performed essentially as previously described.[57] Binding was determined indirectly by the ability of compounds to compete with 50 pM [^{3}H]-(*R*)-quinuclidinyl benzilate in a suspension of brain membranes. Nonspecific binding was evaluated by the inclusion of 1000-fold excess atropine in a separate set of samples. IC_{50} values were determined from Hill plots of the inhibition data and are reported as means ± sem of three independent experiments performed in triplicate.

Phosphoinositide Metabolism in Rat Cortical Slices. The methods were modified from those described by Brown et al.[58] as previously reported.[59,60] The cerebral cortex was dissected according to the method of Glowinski and Iversen.[61] In these studies, [^{3}H]inositol was purified prior to use by passing over a Dowex AGI-X8 anion-exchange column to remove charged degradation products of [^{3}H]inositol. The amount of [^{3}H]inositol phosphates formed in the assay was determined essentially according to Wreggett and Irvine[62] except that the separation of inositol phosphates was accomplished using an Amersham Super Separator Manifold.

Cell Culture. A9 L cells were maintained as monolayer cultures in 175 cm^2 polystyrene tissue culture flasks at 37 °C in a humidified atmosphere of 95% air and 5% CO_2. Growth media (DMEM supplemented with 10% fetal bovine serum, 50 units/mL penicillin G and 50 μg/mL streptomycin, and 4 mM L-glutamine) were changed 24 h after each subculture (every third day). Media were sterilized by filtration through 0.2 μm filterware. Cell viability was determined by observing the cells microscopically at a magnification of 100× and through trypan blue exclusion. Living cells were used from passages 20−31 of the A9 L cell line expressing m1 receptors, passages 19−38 of the A9 L cell line expressing m2 receptors, and passages 12−23 of the A9 L cell line expressing m3 receptors.

Membrane Preparation (for Binding Assays). As described previously by Lee and colleagues,[63] cells reaching confluence from two flasks were scraped into 20 mL of cold medium (4 °C) and collected by centrifugation for 10 min at 1600*g* at 4 °C. Cells were washed by resuspension of the cell pellet in 20 mL of ice-cold binding buffer (10 mM HEPES containing 5 mM $MgCl_2$, pH 7.4) and collected by centrifugation for 10 min at 1600*g* at 4 °C. The pellet was resuspended in 5 mL of cold buffer and homogenized for 30 s at setting 8 in a Brinkman Polytron. The resulting suspension was diluted into a volume of 20 mL and centrifuged for 10 min at 1600*g* and 4 °C. The pellet, containing nuclei and large cellular debris, was discarded, and membranes in the supernatant were pelleted for 30 min at 20000*g* and 4 °C. The pellet was suspended in 4 mL of cold buffer and homogenized again. The final membrane preparation was used for radioligand binding assays after its protein concentration was determined through a modified Lowry assay.

[^{3}H]-(*R*)-QNB Saturation Experiments. In a fashion similar to the procedure described by Dörje and colleagues,[64] freshly prepared cell membranes (10−30 μg protein/mL) were incubated in triplicate with increasing concentrations of [^{3}H]-(*R*)-QNB in a final volume of 1 mL at room temperature for 2 h. At each concentration of [^{3}H]-(*R*)-QNB, 5000-fold excess atropine (or L-hyoscyamine) was used to determine nonspecific binding. Membranes with bound [^{3}H]-(*R*)-QNB were collected by filtration through an M-24R Brandel cell harvester onto Whatman GF/C filters. Filters were rinsed twice with 5 mL of ice-cold buffer and transferred to 20 mL scintillation vials. After drying overnight, vials were filled with 5 mL of CytoScint, and the radioactivity of each vial was counted in a TM Analytic β-counter for 2 min at 800 K.

Inhibition Assays for Agonists. Assays were initiated by addition of freshly prepared membranes (30 μg) into triplicate test tubes containing increasing concentrations of unlabeled ligands and one concentration of [^{3}H]-(*R*)-QNB. The concentration of [^{3}H]-(*R*)-QNB was chosen based on the affinity observed in the direct binding assays (30 pM for m1 receptors). A 5000-fold excess concentration of atropine was used to assess nonspecific binding. Incubations were carried out in 1 mL total volume at room temperature for 2 h and were terminated by filtration as described above.

Phosphoinositide Turnover Assays. Intact A9 L cells expressing either m1 muscarinic receptors (from passages 20−30) or m3 receptors (from passages 12−23) were incubated with [^{3}H]-*myo*-inositol (0.5 μCi/well) in 24-well plates with a plating density of 10^5 cells per well. After incubation at 37 °C for 48 h in 0.5 mL of DMEM with 95% air/5% CO_2, the medium was aspirated and the cells were washed twice with 1 mL of EMEM containing 10 mM LiCl. The medium was replaced by 0.5 mL of the same medium containing 10 mM LiCl and incubated at 37 °C for 20 min. The reaction was initiated by the addition of 25 μL of agonist at appropriate concentrations (or medium for determination of basal levels) and allowed to continue for an additional 30 min. For antagonist experiments, atropine was added simultaneously with the agonist.

At the end of the incubation period, the reaction was terminated by aspiration of medium and addition of 0.5 mL of 5% (v/v) ice-cold trichloroacetic acid (TCA). The wells were rinsed with 0.5 mL of distilled H_2O, which was added to the TCA extract. The TCA extract was applied to Dowex-formate columns (Biorad AG1-X8 resin, formate form, 100−200 mesh). The columns were washed three times with 3 mL of 5 mM *myo*-inositol, and then total [^{3}H]inositol phosphates were eluted with 1 mL of 1.0 M ammonium formate/0.1 M formic acid. Then, 0.5 mL of the eluate was counted in 10 mL of CytoScint on a TM Analytic beta counter.

Assays of Cyclic AMP Formation. Measurement of cAMP levels was carried out according to the procedures described by Wess et al.[65] Intact A9 L cells expressing m2 muscarinic receptors (from passages 9−14) were incubated in 24-well plates (at a density of 10^5 cells per well) in DMEM with 95% air/5% CO_2 at 37 °C for 24 h. After incubation, the growth medium was replaced with 250 μL of DMEM containing 1 mM IBMX, 20 mM HEPES, and the appropriate agonist concentrations. The reaction was terminated after a 10-min incubation at room temperature by aspiration of medium and addition of 250 μL of an ice-cold solution containing 0.1 N HCl and 1 mM $CaCl_2$. After 15 min, the solution was aspirated into appropriately labeled tubes and diluted with 250 μL of cAMP assay buffer. The cAMP levels were determined by radioimmunoassay as previously described by Brooker et al.[66] using the nonacetylation protocol as outlined in the Amersham cAMP assay kit. A standard solution of cAMP was prepared by adding 2 mL of deionized water to a stock powder containing 64 pmol of cAMP to obtain a final concentration of 32 pmol/mL in 0.05 M acetate buffer containing 0.01% thimerosal. Serial dilutions of 500 μL/tube were made from the stock solution using the diluted assay buffer (0.05 M acetate buffer, pH 5.8 with 0.01% azide). Aliquots (100 μL) from each serial dilution permitted seven standard levels of cAMP ranging from 25 to 1600 fmol.

Polypropylene tubes were labeled in duplicate for total counts (TC), zero standard tubes (B_o), standards, and samples. Assay buffer (100 μL) was added to the zero standard tubes (B_o). Each standard and the unknown samples (100 μL) were similarly added to the appropriately labeled tubes. [^{125}I]cAMP (100 μL) was added into all tubes followed by 100 μL of antiserum in all tubes except the TC. All samples were vortexed thoroughly, covered with plastic film, and incubated for 3 h at 2−8 °C. After the incubation, Amerlex-M second antibody reagent was added (500 μL) into all tubes except the TC, which was covered and put aside for counting. All the samples were vortexed and incubated for 10 min at room temperature. The antibody bound fraction was separated by centrifugation for 10 min at 1500*g*, decanting the supernatant and allowing the samples to drain for 5 min. The radioactivity in each tube was then determined by counting for 2 min in a gamma scintillation counter (TM Analytic). The results were calculated from the average cpm values for each set of replicate samples and the percent B_o/TC. The percent bound for each standard and sample was also calculated. A standard curve was generated by plotting the percent bound for each concentration of cAMP, and the amount of cAMP (fmol/tube) for each unknown sample was determined. The concentration of (cAMP/mL or cAMP/10^5 cells) was derived using the appropriate dilution factor and correcting for the sample volume assayed.

Data Analysis. All data points were determined in triplicate except where noted and plotted as the mean of at least three independent experiments. Data from [^{3}H]-(*R*)-QNB binding experiments were subjected to a Scatchard analysis and B_{max} and K_d values were determined. Data from each inhibition assay were analyzed by nonlinear regression methods for best fit to single or multiple binding sites. An *F* test was used to determine the model which best fit the experimental data with α set at 0.05. The IC_{50} values and percentages of high-, medium-, and/or low-affinity sites were determined for each ligand. IC_{50} values were converted to K_i values using the Cheng−Prusoff equation.[67]

Data from each PI assay were analyzed by iterative fit to the hyperbolic equation $Y = (S_{max}x)/(x + EC_{50})$. Correlation coefficients were generally >0.95. Values of EC_{50} and S_{max} determined from separate experiments for each agonist were then compared by one-factor analysis of variance, and individual comparisons were made using a Tukey test.

Molecular Modeling and Computational Chemistry. Computational chemical calculations were performed on a VAX 6420 computer running Still's program MacroModel (version 3.0)[47] as outlined in previous studies.[12,60] Conformational minima were generated for the protonated species of arecoline and **1a** using the modified MM2 and AMBER force fields and parameters as implemented in the program. Torsional angles were explored in 30° increments over the full 360° circle and the resulting structures then fully minimized to a final RMS gradient of <0.005 kJ/Å by using the full-matrix Newton−Raphson method. Structures **2a** and **4** were modeled using similar methods, except that, due to the absence of 1,2,4-oxadiazole parameters in the MM2 force field, a carbon atom was substituted for the ring oxygen to conduct a multiconformer search as described above. The oxygen was then reinserted for subsequent molecular orbital calculations as outlined below.

MacroModel files generated from MM2 calculations were used as input files for Dewar's MNDO methodology[68] implemented in the program MOPAC.[69] Refined geometries and partial atomic charges were generated within MOPAC. Output files then were viewed using the MacroModel graphics subroutine.

Docking studies were initiated on a Silicon Graphics Indigo^2 workstation using MacroModel (version 4.5),[48] Sybyl (version 6.1),[54] and MOPAC (version 6.0) software, employing the model of the m1 muscarinic receptor devised by Nordvall and Hacksell.[50] The model of the m1 receptor site was modified to show connectivity to a polypeptide backbone, and charges were added using the semiempirical method AM1, which describes hydrogen bond systems well.[70] The charges on each ligand were added in a similar fashion.

Each conformation of the ligands was docked onto the receptor site, i.e. was fitted into the m1 receptor model. The use of the TRIPOS forcefield (as implemented in the program Sybyl) was necessary in order to obtain the oxadiazole parameters. Throughout the process, internal energy changes for the ligands and intermolecular steric and electrostatic energy terms between the elements of the dimer were considered, keeping the geometry of the site rigid. Each minimized ligand conformation was rotated by 90° increments about the C5−C bond to find different starting positions for docking studies. The resulting structures were ranked in order of increasing energy, and potential H-bonding interactions were examined within Sybyl.

Acknowledgment. The work was supported by NIH research grants NS 01493 and NS 31173, by a Research Challenge grant from the Ohio Board of Regents, and by the DeArce Memorial Endowment Fund. The authors are grateful to Drs. Wayne P. Hoss and Graham J. Durant for their contributions to the work outlined here. Also, the authors thank Dr. Doug Gage of Michigan State University and Dr. Sharad Magar for obtaining mass spectral data.

References

(1) Davies, P.; Maloney, A. J. F. Selective loss of central cholinergic neurons in Alzheimer's disease. *Lancet* **1976**, No. 2, 1403.
(2) Whitehouse, P. J.; Martino, A. M.; Antuono, P. G.; Lowenstein, P. R.; Coyle, J. T.; DeLong, M. R. Alzheimer's disease and senile dementia: loss of neurons in the basal forebrain. *Science* **1982**, *215*, 1237−1239.
(3) Coyle, J. T.; Price, D. L.; DeLong, M. R. Alzheimer's disease: A disorder of cortical cholinergic innervation. *Science* **1983**, *219*, 1184−1190.
(4) Soininen, H.; Kosunen, O.; Helisalmi, S.; Mannermaa, A.; Paliärvi, L.; Talasniemi, S.; Ryynänen, M.; Riekkinen, P., Sr. A severe loss of choline acetyltransferase in the frontal cortex of Alzheimer patients carrying apolipoprotein ϵ4 allele. *Neurosci. Lett.* **1995**, *187*, 79−82.
(5) Christie, J. E.; Shering, A.; Ferguson, J.; Glen, A. I. M. Physostigmine and arecoline. Effects of intravenous infusions in Alzheimer presenile dementia. *Br. J. Psychiatry* **1981**, *138*, 46−50.
(6) Summers, W. K.; Majovski, L. V.; Marsh, G. M.; Tachiki, K.; Kling, A. Oral tetrahydroaminoacridine in long-term treatment of senile dementia, Alzheimer type. *N. Engl. J. Med.* **1986**, *315*, 1241−1245.
(7) Hollander, E.; Mohs, R. C.; Davis, K. L. Cholinergic approaches to the treatment of Alzheimer's disease. *Br. Med. Bull.* **1986**, *42*, 97−100.
(8) Moos, W.; Davis, R. E.; Schwarz, R. D.; Gamzu, E. R. Cognition activators. *Med. Res. Rev.* **1988**, *8*, 353−391.
(9) Wamsley, J. K.; Gehlert, D. R.; Roeske, W. R.; Yamamura, H. I. Muscarinic antagonist binding site heterogeneity as evidenced by autoradiography after direct labeling with [^{3}H]-QNB and [^{3}H]-pirenzepine. *Life Sci.* **1984**, *34*, 1395−1402.
(10) Mash, D. C.; Potter, L. T. Autoradiographic localization of M1 and M2 muscarine receptors in the rat brain. *Neuroscience* **1986**, *19*, 551.
(11) Cortés, R.; Palacios, J. M. Muscarinic cholinergic receptor subtypes in the rat brain. I. Quantitative autoradiographic studies. *Brain Res.* **1986**, *362*, 227−238.
(12) Messer, W. S., Jr.; Ellerbrock, B. R.; Smith, D. A.; Hoss, W. Regional differences in the binding of selective muscarinic antagonists to rat brain: Comparison with minimum energy conformations. *J. Med. Chem.* **1989**, *32*, 1164−1172.
(13) Buckley, N. J.; Bonner, T. I.; Brann, M. R. Localization of a family of muscarinic receptor mRNAs in rat brain. *J. Neurosci.* **1988**, *8*, 4646−4652.
(14) Wall, S. J.; Yasuda, R. P.; Hory, F.; Flagg, S.; Martin, B. M.; Ginns, E. I.; Wolfe, B. B. Production of antisera selective for m1 muscarinic receptors using fusion proteins: Distribution of m1 receptors in rat brain. *Mol. Pharmacol.* **1991**, *39*, 643−649.
(15) Caulfield, M. P.; Higgens, G. A.; Straughan, D. W. Central administration of the muscarinic receptor subtype-selective antagonist pirenzepine selectively impairs passive avoidance learning in the mouse. *J. Pharm. Pharmacol.* **1983**, *35*, 131−132.
(16) Hagan, J. J.; Jansen, J. H. M.; Broekkamp, C. L. E. Blockade of spatial learning by the M_1 muscarinic antagonist pirenzepine. *Psychopharmacology* **1987**, *93*, 470−476.
(17) Messer, W. S., Jr.; Thomas, G. J.; Hoss, W. P. Selectivity of pirenzepine in the central nervous system. II. Differential effects of pirenzepine and scopolamine on performance of a representational memory task. *Brain Res.* **1987**, *407*, 37−45.
(18) Messer, W. S., Jr.; Bohnett, M.; Stibbe, J. Evidence for a preferential involvement of M_1 muscarinic receptors in representational memory. *Neurosci. Lett.* **1990**, *116*, 184−189.
(19) Gil, D. W.; Wolfe, B. B. Pirenzepine distinguishes between muscarinic receptor-mediated phosphoinositide breakdown and inhibition of adenylate cyclase. *J. Pharmacol. Exp. Ther.* **1985**, *232*, 608−616.
(20) Fisher, S. K.; Figueiredo, J. C.; Bartus, R. T. Differential stimulation of inositol phospholipid turnover in brain by analogs of oxotremorine. *J. Neurochem.* **1984**, *43*, 1171−1179.
(21) Fisher, S. K.; Agranoff, B. W. Receptor activation and inositol lipid hydrolysis in neural tissues. *J. Neurochem.* **1987**, *48*, 999−1017.
(22) Mash, D. C.; Flynn, D. D.; Potter, L. T. Loss of M2 muscarine receptors in the cerebral cortex in Alzheimer's disease and experimental cholinergic denervation. *Science* **1985**, *228*, 1115−1117.
(23) Lapchak, P. A.; Araujo, D. M.; Quirion, R.; Collier, B. Binding sites for 3H-AF-DX 116 and effect of AF-DX 116 on endogenous acetylcholine release from rat brain slices. *Brain Res.* **1989**, *496*, 285−294.
(24) Hoss, W.; Messer, W. S., Jr.; Monsma, F. J., Jr.; Miller, M. D.; Ellerbrock, B. R.; Scranton, T.; Ghodsi-Hovsepian, S.; Price, M. A.; Balan, S.; Mazloum, Z.; Bohnett, M. Biochemical and behavioral evidence for muscarinic autoreceptors in the CNS. *Brain Res.* **1990**, *517*, 195−201.
(25) Richards, M. H. Rat hippocampal muscarinic autoreceptors are similar to the M2 (cardiac) subtype − Comparison with hippocampal M1, atrial M2 and ileal M3 receptors. *Br. J. Pharmacol.* **1990**, *99*, 753−761.

(26) Hammer, R.; Giraldo, E.; Schiavi, G. B.; Monferini, E.; Ladinsky, H. Binding profile of a cardioselective muscarine receptor antagonist, AF-DX 116, to membranes of peripheral tissues and brain in the rat. *Life Sci.* **1986**, *38*, 1653−1662.
(27) Peralta, E. G.; Ashkenazi, A.; Winslow, J. W.; Smith, D. H.; Ramachandran, J.; Capon, D. J. Distinct primary structures, ligand-binding properties and tissue-specific expression of four human muscarinic acetylcholine receptors. *EMBO J.* **1987**, *6*, 3923−3929.
(28) Wall, S. J.; Yasuda, R. P.; Li, M.; Wolfe, B. B. Development of an antiserum against m3 muscarinic receptors − Distribution of m3-receptors in rat tissues and clonal cell lines. *Mol. Pharmacol.* **1991**, *40*, 783−789.
(29) Messer, W. S., Jr.; Dunbar, P. G.; Rho, T.; Periyasamy, S.; Ngur, D.; Ellerbrock, B. R.; Bohnett, M.; Ryan, K.; Durant, G. J.; Hoss, W. Synthesis, biochemical activity and behavioral effects of a series of 1,4,5,6-tetrahydropyrimidines as novel ligands for M_1 receptors. *Bioorg. Med. Chem. Lett.* **1992**, *2*, 781−786.
(30) Dunbar, P. G.; Durant, G. J.; Fang, Z.; Rho, T.; Abuh, Y. F.; El-Assadi, A. A.; Ngur, D.; Periyasamy, S.; Hoss, W.; Messer, W. S., Jr. Design, synthesis, and neurochemical evaluation of 5-(3-alkyl-1,2,4-oxadiazol-5-yl)-1,4,5,6-tetrahydropyrimidines as M_1 receptor agonists. *J. Med. Chem.* **1993**, *36*, 842−847.
(31) Dunbar, P. G.; Durant, G. J.; Rho, T.; Ojo, B.; Huzl, J. J., III; Smith, D. A.; El-Assadi, A. A.; Sbeih, S.; Ngur, D. O.; Periyasamy, S.; Hoss, W.; Messer, W. J., Jr. Design, synthesis, and neurochemical evaluation of 2-amino-5-(alkoxycarbonyl)-3,4,5,6-tetrahydropyridines and 2-amino-5-(alkoxycarbonyl)-1,4,5,6-tetrahydrohydropyrimidines as M_1 muscarinic receptor agonists. *J. Med. Chem.* **1994**, *37*, 2774−2782.
(32) Hirotsu, T.; Katoh, S.; Sugasaka, K.; Seno, M.; Itagaki, T. Binding ability of acetamide oxime with proton, copper (II) and dioxouranium (VI) in aqueous solutions. *J. Chem. Soc., Dalton Trans.* **1986**, 1609.
(33) Bandsma, L. In *Acetylenic Chemistry*, 2nd ed.; Elsevier Press: New York, 1988; pp 217−280.
(34) Evans, R. F.; Shannon, J. S. Hydropyrimidies. 4. Catalytic reduction of substituted pyrimidines. *J. Chem. Soc.* **1965**, 1406−1412.
(35) Spry, D. O.; Aaron, H. S. 5-Hydroxytetrahydropyrimidine and its 2-methyl homolog. *J. Org. Chem.* **1966**, *31*, 3838−3839.
(36) Tecle, H.; Lauffer, D. J.; Mirzadegan, T.; Moos, W. H.; Moreland, D. W.; Pavia, M. R.; Schwarz, R. D.; Davis, R. E. A rationale for the design and synthesis of m1 selective muscarinic agonists. *Bioorg. Med. Chem. Lett.* **1992**, *2*, 821−826.
(37) Tecle, H.; Lauffer, D. J.; Mirzadegan, T.; Moos, W. H.; Moreland, D. W.; Pavia, M. R.; Schwarz, R. D.; Davis, R. E. Synthesis and SAR of bulky 1-azabicyclo[2.2.1]-3-one oximes as muscarinic receptor subtype selective agonists. *Life Sci.* **1993**, *52*, 505−511.
(38) Brann, M. R.; Buckley, N. J.; Jones, P.; Bonner, T. I. Expression of a cloned muscarinic receptor in A9 L cells. *Mol. Pharmacol.* **1987**, *32*, 450−455.
(39) Potter, L. T.; Ferrendelli, C. A. Affinities of different cholinergic agonists for the high and low affinity states of the hippocampal M1 muscarine receptors. *J. Pharmacol. Exp. Ther.* **1989**, *248*, 974−978.
(40) Bujo, H.; Nakai, J.; Kubo, T.; Fukuda, K.; Akiba, I.; Maeda, A.; Mishina, M.; Numa, S. Different sensitivities to agonist of muscarinic acetylcholine receptor subtypes. *FEBS Lett.* **1988**, *240*, 95−100.
(41) Schwarz, R. D.; Davis, R. E.; Jaen, J. C.; Spencer, C. J.; Tecle, H.; Thomas, A. J. Characterization of muscarinic agonists in recombinant cell lines. *Life Sci.* **1993**, *52*, 465−472.
(42) Fisher, S. K.; Klinger, P. D.; Agranoff, B. W. Muscarinic agonist binding and phospholipid turnover in brain. *J. Biol. Chem.* **1983**, *258*, 7358−7363.
(43) Fisher, S. K.; Snider, R. M. Differential receptor occupancy requirements for muscarinic cholinergic stimulation of inositol lipid hydrolysis in brain and in neuroblastomas. *Mol. Pharmacol.* **1987**, *32*, 81−90.
(44) Periyasamy, S.; Messer, W. S., Jr.; Rocknich, S.; Hoss, W. Alkoxy-1,2,5-thiadiazole derivatives of arecoline stimulate M1 muscarinic receptors coupled to phosphoinositide turnover. *Brain Res.* **1995**, *693*, 118−123.
(45) Novotny, E. A.; Brann, M. R. In *Fourth International Symposium on Subtypes of Muscarinic Receptors*; Elsevier Trends Journals: Wiesbaden, FRG, 1989; p 116.
(46) Olianas, M. C.; Onali, P.; Neff, N. H.; Costa, E. C. Adenylate cyclase activity of synaptic membranes from rat striatum. Inhibition by muscarinic receptors. *Mol. Pharmacol.* **1983**, *23*, 393−398.
(47) Lipton, M.; Still, W. C. The multiple minimum problem in molecular modeling. Tree searching internal coordinate conformational space. *J. Comput. Chem.* **1988**, *9*, 343−355.
(48) Mohamadi, F.; Richards, N. G. J.; Guida, W. C.; Liskamp, R.; Lipton, M.; Caufield, C.; Chang, G.; Hendrickson, T.; Still, W. C. Macromodel-An integrated software system for modeling organic and bioorganic molecules using molecular mechanics. *J. Comput. Chem.* **1990**, *11*, 440.
(49) Ojo, B.; Dunbar, P. G.; Durant, G. J.; Nagy, P. I.; Huzl, J. J., III; Periyasamy, S.; Ngur, D. O.; El-Assadi, A. A.; Hoss, W. P.; Messer, W. S., Jr. Synthesis and biochemical activity of novel amidine derivatives as m1 muscarinic receptor agonists. *Bioorg. Med. Chem.* **1996**, *4*, 1605−1615.
(50) Nordvall, G.; Hacksell, U. Binding-site modeling of the muscarinic m1 receptor − a combination of homology-based and indirect approaches. *J. Med. Chem.* **1993**, *36*, 967−976.
(51) Wess, J.; Maggio, R.; Palmer, J. R.; Vogel, Z. Role of conserved threonine and tyrosine residues in acetylcholine binding and muscarinic receptor activation. A study with m3 muscarinic receptor point mutants. *J. Biol. Chem.* **1992**, *267*, 19313−19319.
(52) Bluml, K.; Mutschler, E.; Wess, J. Functional role in ligand binding and receptor activation of an asparagine residue present in the sixth transmembrane domain of all muscarinic receptors. *J. Biol. Chem.* **1994**, *269*, 18870−18876.
(53) Ward, J. S.; Merritt, L.; Klimkowski, V. J.; Lamb, M. L.; Mitch, C. H.; Bymaster, F. P.; Sawyer, B. D.; Shannon, H. E.; Olesen, P. H.; Honoré, T.; Sheardown, M. J.; Sauerberg, P. Novel functional M_1 selective muscarinic agonists. II. Synthesis and structure-activity relationships of 3-(pyrazinyl)-1,2,5,6-tetrahydro-1-methylpyridines. Construction of a molecular model for the M_1 pharmacophore. *J. Med. Chem.* **1992**, *35*, 4011−4019.
(54) TRIPOS, Inc., St. Louis, MO, 1994.
(55) Sauerberg, P.; Olesen, P. H.; Nielsen, S.; Treppedahl, S.; Sheardown, M. J.; Honoré, T.; Mitch, C. H.; Ward, J. S.; Pike, A. J.; Bymaster, F. P.; Sawyer, B. D.; Shannon, H. E. Novel functionally selective M_1 muscarinic agonists. Synthesis and structure-activity relationships of 3-(1,2,5-thiadiazolyl)-1,2,5,6-tetrahydro-1-methylpyridines. *J. Med. Chem.* **1992**, *35*, 2274−2283.
(56) Grochowski; Jurczac. New synthesis of O-alkylhydroxylamines. *Synthesis* **1976**, *10*, 682−684.
(57) Farrar, J. R.; Hoss, W.; Herndon, R. M.; Kuzmiak, M. Characterization of muscarinic cholinergic receptors in the brains of copper deficient rats. *J. Neurosci.* **1985**, *5*, 1083−1089.
(58) Brown, E.; Kendall, D. A.; Nahorski, S. R. Inositol phospholipid hydrolysis in rat cerebral cortical slices: I. Receptor characterisation. *J. Neurochem.* **1984**, *42*, 1379−1387.
(59) Periyasamy, S.; Hoss, W. Kappa opioid receptors stimulate phosphoinositide turnover in rat brain. *Life Sci.* **1990**, *47*, 219−225.
(60) Hoss, W.; Woodruff, J. M.; Ellerbrock, B. R.; Periyasamy, S.; Ghodsi-Hovsepian, S.; Stibbe, J.; Bohnett, M.; Messer, W. S., Jr. Biochemical and behavioral responses of pilocarpine at muscarinic receptor subtypes in the CNS. Comparison with receptor binding and low-energy conformations. *Brain Res.* **1990**, *533*, 232−238.
(61) Glowinski, J.; Iversen, L. L. Regional studies of catecholamines in rat brain I: the disposition of [^{3}H]norepinephrine, [^{3}H]-dopamine and [^{3}H]dopa in various regions of the brain. *J. Neurochem.* **1966**, *13*, 655−669.
(62) Wreggett, K. A.; Irvine, R. F. A rapid separation method for inositol phosphates and their isomers. *Biochem. J.* **1987**, *245*, 655−660.
(63) Lee, N. H.; El-Fakahany, E. E. Allosteric interactions at the m1, m2 and m3 muscarinic receptor subtypes. *J. Pharmacol. Exp. Ther.* **1991**, *256*, 468−470.
(64) Dörje, F.; Wess, J.; Lambrecht, G.; Tacke, R.; Mutschler, E.; Brann, M. R. Antagonist binding profiles of five cloned human muscarinic receptor subtypes. *J. Pharmacol. Exp. Ther.* **1991**, *256*, 727−733.
(65) Wess, J.; Bonner, T. I.; Dörje, F.; Brann, M. R. Delineation of muscarinic receptor domains conferring selectivity of coupling to guanine nucleotide-binding proteins and second messengers. *Mol. Pharmacol.* **1990**, *38*, 517−523.
(66) Brooker, G.; Harper, J. F.; Teraski, W. L.; Moylan, R. D. Radioimmunoassay of cyclic AMP and cyclic GMP. *Adv. Cycl. Nucleotide Res.* **1979**, *10*, 1−33.
(67) Cheng, Y.-C.; Prusoff, W. H. Relationship between the inhibition constant (K_i) and the concentration of inhibitor which causes 50 per cent inhibition (I_{50}) of and enzymatic reaction. *Biochem. Pharmacol.* **1973**, *22*, 3099−3108.
(68) Dewar, M. J. S.; Thiel, W. Ground states of molecules. The MNDO method. Approximations and parameters. *J. Am. Chem. Soc.* **1977**, *99*, 4899−4907.
(69) Stuart, J. J. P. QCPE no. 455, Bloomington, IN.
(70) Dewar, M. J. S.; Zoebisch, E. G.; Healy, E. F.; Stuart, J. J. P. AM1: A new general purpose quantum mechanical molecular model. *J. Am. Chem. Soc.* **1985**, *107*, 3902−3909.

JM960467D